Multiscale Modeling: A Review

By Mark Horstemeyer

***Practical Aspects of Computational Chemistry*, ed. J. Leszczynski and M.K. Shukla, Springer Science+Business Media, pp. 87-135, 2009.**

Department of Mechanical Engineering, Mississippi State University, Mississippi 39760, USA

Abstract

This review of multiscale modeling covers a brief history of the various multiscale methodologies related to solid materials and the associated experimental influences, the various influence of multiscale modeling on different disciplines, and some examples of multiscale modeling in design of structural components. Although computational multiscale modeling methodologies have been developed in the very late 20th century, the fundamental notions of multiscale modeling have been around since da Vinci studied different sizes of ropes. The recent rapid growth in multiscale modeling arose from the confluence of parallel computing power, experimental capabilities to characterize structure-property relations down to the atomic level, and theories that admit multiple length scales. The ubiquitous research focus in multiscale modeling has broached different disciplines (solid mechanics, fluid mechanics, materials science, physics, mathematics, biological, and chemistry), different regions of the world (most continents), and different length scales (from atoms to autos).

Keywords

Hierarchical multiscale modeling, concurrent multiscale modeling, internal state variables, constitutive model, fracture, damage, inelasticity

1. Introduction

The recent surge of multiscale modeling related to solid mechanics that has now grown into an international multidisciplinary activity and has broached almost every industry was birthed from an unlikely source. Because the US Department of Energy (DOE) national labs started to reduce nuclear underground tests in the mid 1980's, with the last one in 1992, the idea of simulation based design and analysis concepts were birthed and multiscale modeling was a key in garnering more precise and accurate predictive tools. In essence, the number of large scale systems level tests that were previously used to validate a design was reduced to nothing thus warranting the increase in simulation results of the complex systems for design verification and validation purposes.

Essentially, the idea of filling the space of system level "tests" was then proposed to be filled by simulation results. After the Comprehensive Test Ban Treaty of 1996, in which many countries pledged to discontinue all systems level nuclear testing, programs like the Advanced Strategic Computing Initiative (ASCI) were birthed within the Department of Energy (DOE) and managed by the national labs within the US. Within ASCI, the basic recognized premise was to provide more accurate and precise simulation based design and analysis tools. Because of the requirements for greater complexity in the simulations, parallel computing and multiscale modeling became the major challenges that needed to be addressed. With this perspective the idea of experiments shifted from the large scale complex tests to multiscale experiments that provided material models with validation at different length scales. If the simulations were

physically based and less empirical, then a predictive capability could be realized. As such, various multiscale modeling methodologies were independently being created at the DOE national labs: Los Alamos National Lab (LANL), Lawrence Livermore National Laboratory (LLNL), Sandia National Laboratories (SNL), and Oak Ridge National Laboratory (ORNL). In addition, personnel from these national labs encouraged, funded, and managed academic researched related to multiscale modeling. Hence, the creation of different methodologies and computational algorithms for parallel environments gave rise to different emphases regarding multiscale modeling and the associated multiscale experiments.

The advent of parallel computing also contributed to the development of multiscale modeling. Because more degrees of freedom could be resolved by parallel computing environments, more accurate and precise algorithmic formulations could be admitted. This thought also drove the political leaders to encourage the simulation-based design concepts.

At LANL, LLNL, and ORNL the multiscale modeling efforts were driven from the materials science and physics communities with a bottom-up approach. Each had different programs that tried to unify computational efforts, materials science information, and applied mechanics algorithms with different levels of success. Multiple scientific articles were written, and the multiscale activities took different lives of their own. At SNL, the multiscale modeling effort was an engineering top-down approach starting from continuum mechanics perspective, which was already rich with a computational paradigm. SNL tried to merge the materials science community into the continuum mechanics community to address the lower length scale issues that could help solve engineering problems in practice.

Once this management infrastructure and associated funding was in place at the various DOE institutions, different academic research projects started, initiating various satellite networks of multiscale modeling research. This technological transfer also arose into other labs within the Department of Defense and industrial research communities.

The growth of multiscale modeling in the industrial sector was primarily due to financial motivations. From the DOE national labs perspective, the shift from large scale systems experiments mentality occurred because of the 1996 Nuclear Ban Treaty. Once industry realized that the notions of multiscale modeling and simulation based design were invariant to the type of product, and that effective multiscale simulations could in fact lead to design optimization, a paradigm shift began to occur, in various measures within different industries, as cost savings and accuracy in product warranty estimates were rationalized. Whether designing an automobile, airplane, building, or any structural system for that matter, large scale systems tests were (and are) expensive, and cost models showed that a physics-based design can give a great return on investment. The advantages include the following:

1. Multiscale modeling can reduce the product development time by alleviating costly trial-and error iterations.
2. Multiscale modeling can reduce product costs through innovations in material, product, and process designs.
3. Multiscale modeling can reduce the number of costly large systems scale experiments.
4. Multiscale modeling can increase product quality and performance by providing more accurate predictions of response to design loads.
5. Multiscale modeling can help develop new materials.
6. Multiscale modeling can help medical practice in making diagnostic and prognostic evaluations related to the human body.

Hence, the market drivers for such an explosion of multiscale modeling into various industrial sectors are being realized.

2. Multiscale Modeling Publications

Based on the recent ISI Web of Knowledge (http://www.isiwebofknowledge.com/) Figure 1 illustrates the increasing trend of papers that have been published with "Multiscale Modeling" in the title. Certainly a multiscale modeling article does not need to have these two particular words in the title of the article, but this trend illustrates the rapid growth in the area.

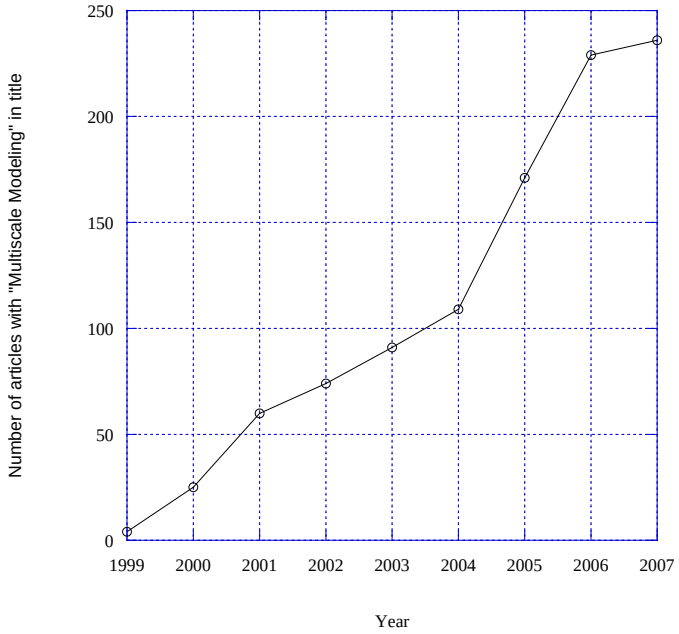

Fig. 1. Number of journal articles published with "Multiscale Modeling in the title. Note the recent trend since 1999 shows a large growth rate.

These articles have been distributed in particular disciplines although the nature of multiscale modeling is really interdisciplinary. The ISI Web of Knowledge shows that the largest number of multiscale modeling articles arose from the Materials Science community followed by the Meteorological and Atmospheric community. The next two disciplines are the Mechanics and Mathematics communities followed by Physics, Electrical Engineering, and Chemistry (and chemical engineering). Other disciplines have produced multiscale modeling articles but to a much lesser degree.

Because of the interdisciplinary nature of multiscale modeling, several new journals have arisen to allow for a venue of presentation that has historically not been a focus of stovepiped disciplines. One journal is the *Multiscale Modeling and Simulation: A SIAM Interdisciplinary Journal* (http://www.siam.org/journals/mms.php), which has given attention to communication bridges between mathematics, chemistry, physics, engineering, computer science, and environmental sciences. Another recent journal is the *International Journal for Multiscale Computational Engineering* (http://www.begellhouse.com/journals/61fd1b191cf7e96f.html), which focuses mainly on algorithm developments although other multiscale issues have been addressed. In 1998, *Physical Mesomechanica* began in Russia to address multilevel issues related to plastic flow [1]. A recent journal is the International *Journal of Theoretical International Journal of Theoretical and Applied Multiscale Mechanics* (http://www.inderscience.com/browse/index.php?journalCODE=ijtamm), which focuses on constitutive modeling issues between size scales and domains. Although other journals, before

these were created, had admitted articles on multiscale modeling, the reviews were typically critical as no appreciation of bridging methodologies were given much credence.

Although multiscale modeling has broached many disciplines, this review will focus on solid materials as described below. As a former manager of the computational fluids dynamic group at Sandia National Labs, the author readily recognizes many areas in which multiscale modeling has affected fluids, for example, in polymer flows, turbulence modeling, weather analysis, etc. However, for brevity's sake the focus here will be on multiscale modeling of solids.

3. Bridging Between Scales: A Difference of Disciplines

Synergy/systems thinking and interdisciplinary thinking brings about the whole being greater than the sum of the parts. Multiscale modeling requires that several disciplines interact, which has led to miscommunications and misunderstandings between communities about what multiscale modeling really is, particularly when one discusses the bridging methodology between length scales.

Clearly, one key in multiscale modeling is the notion of the bridging. Without officially stating the bridging methodology, each discipline has its own methods. Before we discuss each discipline's bridging paradigm, let us consider an analogy of the Brooklyn Bridge in New York versus the Golden Gate Bridge in San Francisco. If one were to just translate the Brooklyn Bridge to San Francisco and call it the Golden Gate Bridge, one would find that the old adage of a "square peg in a round hole" fits. The Golden Gate Bridge required a different design than the Brooklyn Bridge, because of what was required on each side of the bridge and the environments that must be sustained. In other words, the boundary conditions played a major role in the design of the bridge. The same notion needs to be considered when developing bridges for multiscale modeling between different length scales. However, the different research disciplines (materials science, applied mechanics, atmospheric sciences, etc.) tend to focus on the research at each pertinent length scale and not so much the bridge. In fact, modern computational tools at each length scale were just recently published in Yip's [2] Handbook of Materials Modeling, which provides a thorough review of a wide variety of current tools; however, this work did not really deal with bridging methodologies.

In the next sections, the multiscale modeling methods are presented from the different disciplines perspectives. Clearly one could argue that overlaps occur, but the idea here is to present the multiscale methods from the paradigm from which they started. For example, the solid mechanics internal state variable theory includes mathematics, materials science, and numerical methods. However, it clearly started from a solid mechanics perspective and the starting point for mathematics, materials science, and numerical methods has led to other different multiscale methods.

3.1 Solid Mechanics Bridging (Hierarchical Methods)

Inherent within the idea of multiscale modeling is the bridging methodology and the associated length scale of the feature that is required to gain the accurate physics required for the engineering problem [3]. To decide on the pertinent length scale feature of importance, one must consider that in modern solid mechanics, continuum theories are driven by the conservation laws (mass, momentum, and energy); however, there are too many unknowns than the number of equations, so constitutive relations (sometimes erroneously called "laws") are required to solve the set of differential equations for finite element or finite difference analysis (most modern solid mechanics tools employ finite element analysis). When developing a multiscale modeling methodology for the constitutive relations, the kinetics, kinematics, and

thermodynamics need to be consistent in the formulation. There are also certain classical postulates in continuum theory that guide the development of the constitutive theory (objectivity, physical admissibility, equipresence, and locality). Multiscale modeling has been driven by the physical admissibility postulate even at the expense of the postulates of equipresence and locality. Physical admissibility essentially means identifying the physical mechanism or discrete microstructural feature at the particular length scale that is a root source of the phenomenological behavior.

Two different general multiscale methodologies exist starting from the solid mechanics continuum theory paradigm: hierarchical and concurrent. The key difference is the bridging methodology. In concurrent methods, the bridging methodology is numerical or computational in nature. In the hierarchical methods, numerical techniques are independently run at disparate length scales. Then, a bridging methodology such as statistical analysis methods, homogenization techniques, or optimization methods can be used to distinguish the pertinent cause-effect relations at the lower scale to determine the relevant effects for the next higher scale.

One effective hierarchical method for multiscale bridging is the use of thermodynamically constrained internal state variables (ISVs) that can be physically based upon microstructure-property relations. It is a top-down approach, meaning the ISVs exist at the macroscale but reach down to various subscales to receive pertinent information. The ISV theory owes much of its development to the state variable thermodynamics constructed by Helmholtz [4] and Maxwell [5]. The notion of ISV was introduced into thermodynamics by Onsager [6, 7] and was applied to continuum mechanics by Eckart [8, 9].

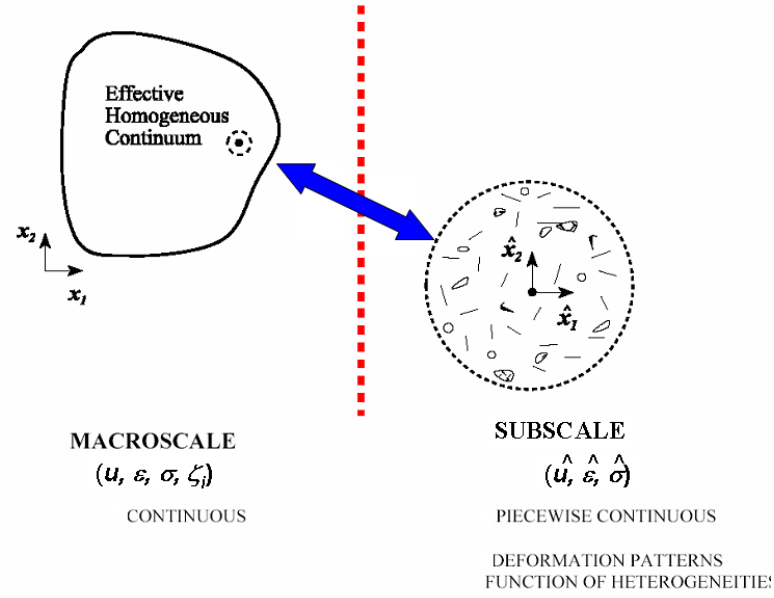

Fig. 2. Homogenization of discretized microstructural features into a continuum medium.

The basic idea behind the theory of ISV is that, in order to uniquely define the Helmholtz free energy [4] of a system undergoing an irreversible process, one has to expand the dimensions of the state space of deformation and temperature (state variables commonly employed in classical thermodynamics to study elastic materials) by introducing a sufficient number of additional state variables which are considered essential for the description of the internal structure with the associated length scales of the material in question. The number of

these ISVs is related to material structure as well as to the degree of accuracy with which one wishes to represent the material response.

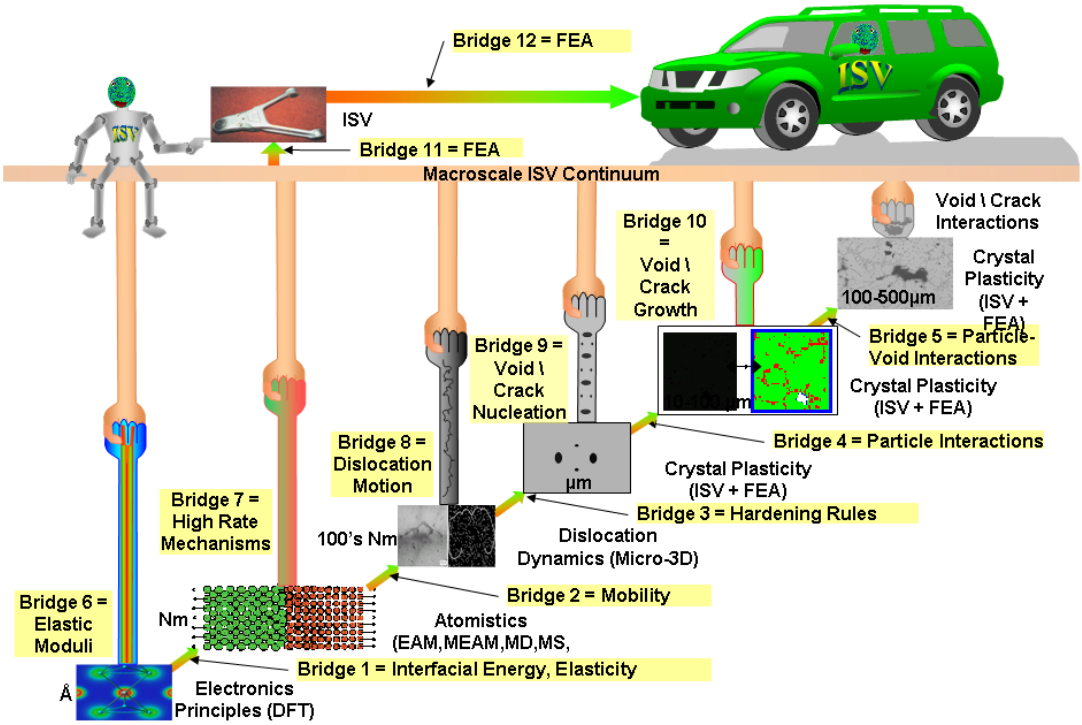

Fig. 3. Multiscale modeling example of a metal alloy used for design in an automotive component. The hierarchical methodology illustrates the different length scale analyses used and various bridges needed. (ISV=internal state variable, FEA=finite element analysis, EAM=Embedded Atom Method, MEAM=Modified Embedded Atom Method, MD=Molecular Dynamics, MS=Molecular Statics, and DFT=Density Functional Theory).

The ISV formulation is a means to capture the effects of a representative volume element and not all of the complex causes at the local level; hence, an ISV will macroscopically average in some fashion the details of the microscopic arrangement. In essence, the complete microstructure arrangement is unnecessary as long as the macroscale ISV representation is complete [10]. Figure 2 illustrates that we can then "average" or "homogenize" the effect of the discrete feature into a continuum that includes a number of ISVs. As a result, the ISV must be based on physically observed behavior and constrained by the laws of thermodynamics [11]. Rice [12] and Kestin and Rice [13] added the notions of inelastic behavior into the context of ISV theory. The inelastic behavior of importance to design and analysis of metal structural components is typically plasticity, damage, and failure. For inelastic dissipative materials, the ISVs relate microstructural characteristics to mechanical behavior and have been used in various materials, polymers, composites, and ceramics [14-19]. However, it may be argued that ISV theory has probably had its greatest impact on metals. In the US, ISV theories have enjoyed success in solving practical engineering problems. The Mechanical Threshold Stress (MTS) Model [20-22] was developed at Los Alamos National Laboratory, and focused on the microstructural details in relation to mechanical properties. Freed [23] at NASA developed an ISV model under the paradigm of unified-creep-plasticity modeling. Bammann [24,25] at Sandia National Laboratories developed an ISV modeling framework that was microstructurally based and fit into the unified-creep-plasticity paradigm. In Europe, Chaboche [26] focused on fatigue, large strain plasticity, and damage in his ISV formulations. Although many other ISV

models could be discussed here, the above-mentioned theories have been successfully used in engineering practice on a routine basis for design and manufacturing for metal and polymer-based material systems.

Not only is ISV theory important from a top-down approach but the linking between scales is critical as well as the different computational methods that can be employed. Figure 3 shows a hierarchical multiscale modeling methodology illustrating the different bridges and analyses required to capture the pertinent plasticity, damage, and failure aspects of metal alloys for use in design of an automotive component. An example will be presented later which describes these different size scale analyses and their associated bridges will be presented.

Before the term multiscale modeling was in vogue, methods of bridging lower length information into a continuum at a higher length scale was being addressed in the solid mechanics community. Eshelby [27, 28] essentially birthed the modern "micromechanics" world of analysis, modeling, and simulation by asserting a "self-consistent" theme. Essentially, subscale hetereogeneities could be assigned an effect within the continuum. The continuum could be assigned as an element, a "Representative Volume Element" or RVE. As such, the composites, metallurgical and applied mechanics communities used this framework for different applications. Modern mixture theory, mean field theory [29], crystal plasticity, Method-of-Cells, Mura-Tanaka Method [30], Homogenization Theory, and the Generalized Method-of-Cells were birthed from the self-consistent Eshelby formulation. Mura [31], Budiansky [32], and Nemat-Nasser and Lori [33] gave a thorough review of these micromechanical self-consistent methods.

A part of the self-consistent method is determining what the RVE should be and how the boundary conditions do work down from higher scales to lower scales. Fairly recently, Gokhale and Yang [34] performed a hierarchical multiscale modeling study examining different length scale microstructures with digital imaging methods and finite element analysis. The technique brought together effects of features at higher length damage evolution and local fracture processes occurring at lower length scales. Hao et al. [35] also employed hierarchical fracture methods at different scales.

In finalizing this section, it is worth noting that aside from the modern-day multiscale modeling using ISV theory and self-consistent theories, determining the length scale effects on mechanics properties has been around a long time and has been summarized by Bazant and Chen [36]. DaVinci in the 1500's made the statement that a longer rope with equal thickness compared to a smaller diameter rope was weaker than the smaller rope. Galileo, in the 1600's, disagreed with DaVinci about the strengths and lengths of ropes as he studied the size effects of bones. Euler in the 1700's related buckling to a column length. In the 1800's, Cauchy related the stress state to radius of a cylinder. In the early 1900's, Bridgman [37] showed on many metal alloys that the notch radii change the stress state of the material. In all of these examples, the length scale parameter was related to the geometry of the component, not to anything internal to the component. Certainly, these types of size scale effects have been a part of modern finite element analysis. However, the multiscale modeling that we are discussing in this review addresses the issues of material micro structural effects on the mechanical properties in the absence and in the presence of these geometrical size scale effects.

3.2 Numerical Methods (Concurrent Methods)

Concurrent methods typically try to combine different scale algorithms together with matching procedures invoked in some overlapping domain in order to resolve the important multiscale physics. A good review of these concurrent methods and the associated challenges can be found in the books of Phillips [38] and Liu et al. [39] and the review articles of Fish [40]

and de Pablo and Curtin [41]. Typical concurrent methods have two different length scales, or at most three different length scales, of interest in the formulations. Too many length scales are cost prohibitive.

The first and most active area of research for concurrent methods has been the coupling of atomistic-level simulations to continuum-level simulations at the same time with different information being shared between the two. The development of fine grid-coarse grid finite element methods [42] was the basis for these different concurrent multiscale methods. For multiscale modeling the fine grid method was traded for other lower length scale methods, such as atomistic methods. For example, Kohlhoff et al. [43, 44] were probably the first to join atomistic level simulations capabilities within a finite element code. Another example was the quasi-continuum approach of Tadmor et al. [45] that came about by joining the physic's community Embedded Atom Method (EAM) molecular statics code developed by Baskes and colleagues [46,47] at Sandia National Labs and the solid mechanics finite element formulations of Ortiz et al. [48]. The notion was to have the atomistic method local to a region where plasticity, fracture, or any activity causing dissipation where the finite element method would apply to the appropriate boundary conditions. Shenoy et al. [49] later applied the quasi-continuum method to interfaces, illustrating an application of a concurrent multiscale modeling can be applied where otherwise single length scale analyses could not address. Miller et al. [50, 51] further extended the concurrent quasi-continuum application space to plasticity and fracture. Shenoy et al. [52] later added an adaptive finite element meshing capability to the quasi-continuum method in order to broaden the application space. At this time Abraham et al. [53] with the help of Plimpton [54] from Sandia National Labs, used an atomistic-finite element code to examine fracture in brittle materials under dynamic loads. There was another group researching concurrent methods at this time as well. Rudd and Broughton [55] and Broughton et al. [56] examined dynamic aspects of concurrent multiscale modeling with atomistics and finite elements and their inherent limitations on particular applications.

Others then went on to study various aspects of quasi-continuum concurrent multiscale methods. Lidirokas et al. [57] studied local stress states around Si nanopixels using this method. Bazant [58] argued that these atomistic-finite element multiscale methods can not really capture inelastic behavior like fracture because the softening effect requires a regularization of the local region that is not resolved.

By the year 2000, the notion of concurrent multiscale modeling had diffused into the greater solid mechanics community at different length scales besides the atomic-continuum level. Shilkrot et al. [59, 60] introduced a method that essentially combines the quasi-continuum method with the discrete dislocation method. In this same spirit, Shiari et al. [61] and Dewald and Curtin [62] connected atomistics with dislocation dynamics simulations in a two-scale methodology to focus on grain boundary effects. At a higher length scale, Zbib and Diaz de la Rubia joined discrete dislocation methods with finite element methods [63]. Hence, the local geometric conditions and kinetics that controlled the dynamics of dislocations were placed into a continuum field theory code that could solve boundary value problems.

Although the crystal plasticity modeling community focused on several length scales in their simulations, the term concurrent multiscale modeling was not historically used. Because crystal plasticity formulations start at the scale of the grain and volume average up to yield polycrystalline results and the polycrystalline results can affect the results within the grain, they are in a sense a pseudo-concurrent method and really a self-consistent method. They can also bring in lower length scale effects in a hierarchical manner [64]. Crystal plasticity models became popular during the 1980s as a tool to study deformation and texture behavior of metals during material processing [65] and shear localization [66,67]. The basic elements of the theory comprise(-s) (i) kinetics related to slip system hardening laws to reflect intragranular work

hardening, including self and latent hardening components [68], (ii) kinematics in which the concept of the plastic spin plays an important role, and (iii) intergranular constraint laws to govern interactions among crystals or grains. The theory is commonly acknowledged for providing realistic prediction/correlation of texture development and stress-strain behavior at large strains as it joins continuum theory with discretized crystal activity.

Similar to crystal plasticity modeling and simulation in which discrete entities such as crystals were placed in a larger continuum domain, Shephard et al. [69] discussed concurrent automatic interacting models at different scales considering geometric representations and discretizations required by microstructure. Still others have focused on the bridging algorithms: the bridging domain method of Xiao and Belytschko [70], the bridging scale method of Wagner and Liu [71], and Karpov et al. [72]. Non-reflecting boundary condition methods originating from the seminal work of Adelman and Doll [73] led to recent works of concurrent multiscale models of Cai et al. [74], Huang and Huang [75], Wagner et al. [76], Karpov et al. [72], and Park et al. [77]. Essentially, the non-reflecting boundary allows for the molecular dynamics (MD) allows for the simulation of a considerably smaller lattice around the local physics of interest, such as a crack tip, while keeping the effects of the eliminated degrees of freedom on the reduced MD system. Also in an effort to address the quasi-statics problem and the dynamics problems discussed by Horstemeyer et al. [78], Fish and Chen [79], and Fish and Yuan [80], which introduced time scale incongruencies along with size scale issues, Klein and Zimmerman [81] developed a concurrent method that could be used in one, two, and three dimensional analysis.

Concurrent multiscale methods have also been employed to address fatigue. Oskay and Fish [82] and Fish and Oskay [83] introduced a nonlocal temporal multiscale model for fatigue based upon homogenization theory. Although these formulations were focused on metals, Fish and Yu [84] and Gal et al. [85] used a similar concurrent multiscale method for analyzing fatigue of composite materials.

3.3 Materials Science Bridging

Perhaps the materials science community has had the greatest impact on modern multicale modeling methods. When addressing the physical admissibility postulate for continuum theory, the materials science community has provided the data. It is inherent within the materials science community to study the various length scale effects, although they have not necessarily focused on multiscale modeling. The terminology typically used in the materials science community is “structure-property” relations. Essentially it is the different structures within the material (grains, particles, defects, inclusions, etc.) that dictate the performance properties of the materials [86, 87].

Different scale features give different scale properties. At the smallest level, the lattice parameter is a key length scale parameter for atomistic simulations. Since atomic rearrangement is intimately related to various types of dislocations, Orowan [88], Taylor [89], Polyani [90], and Nabarro [91] developed a relationship for dislocations that related stress to the inverse of a length scale parameter, the Burgers’ vector [92], which laid the foundation for all plasticity theories. Nabarro [91] also showed that the diffusion rate is inversely proportional to the grain size, another length scale parameter. Hall [93] and Petch [94] related the work hardening rate to the grain size. Ashby [95] found that the dislocation density increased with decreasing second phase particle size. Frank and Read [96-98] showed a relation with a dislocation bowing as a function of spacing distance and size. And Hughes et al. [99,100] discovered that geometrically necessary boundary spacing decreases with increasing strain.

Other experimental studies have revealed that material properties change as a function of size. For example, Fleck et al. [101] have shown in torsion of thin polycrystalline copper wires the normalized yield shear strength increases by a factor of three as the wire diameter is decreased from 100 microns to 12.5 microns. Stolken and Evans [102] observed a substantial increase in hardening during the bending of ultra thin beams. In micro-indentation and nano-indentation tests [103-108], the measured indentation hardness increased by a factor of two as the depth of indentation decreased from 10 microns to 1 micron. When Lloyd [109] investigated an aluminum-silicon matrix reinforced by silicon carbide particles, he observed a significant increase in strength when the particle diameter was reduced from 16 microns to 7.5 microns while holding the particle volume fraction fixed at 15%. Hughes et al. [99,100] investigated deformation induced from frictional loading and found that the stresses near the surface were much greater than that predicted by the local macroscale continuum theory, that is, a length scale dependence was observed. Elssner et al. [110] measured both the macroscopic fracture toughness and the atomic work associated with the separation of an interface between two dissimilar single crystals. The interface (crack tip) between the two materials remained sharp, even though the materials were ductile and contained a large number of dislocations. The stress level necessary to produce atomic decohesion of a sharp interface is on the order of ten times the yield stress, while local theories predict that the maximum achievable stress at a crack tip is no larger than four to five times the yield stress.

In terms of damage/fracture, Griffith [111] found a relation between the crack length and the stress intensity factor. Before this time, Roberts-Austen [112] performed a set of experiments that showed the tensile strength of gold having a strong dependence of the impurity size. Fairly recently, McClintock [113] determined the void growth rates as a function of the void size. Void/Crack nucleation was determined by various aspects of the second phase particle size distribution by Gangalee and Gurland [114]. Horstemeyer et al. [115,116] and Potirniche et al. [117-120] determined the nearest neighbor distance as a length scale parameter for void coalescence modeling for different metals that was experimentally validated by Jones et al. [121]. It is clear that whether damage mechanics or fracture mechanics is employed the length scale of interest is important to model this type of inelastic behavior.

In terms of fatigue, the materials science community has revealed different length scales of interest as well. The idea that local inclusion/defects such as pores, second phase particles, inclusions, and constituents could induce local stress concentrations so the size of the local inclusion/defect could induce local stress concentrations large enough to induce fatigue cracks. Neuber [122] and Peterson [123] clearly showed the relation of notch root sizes on fatigue life. Harkegard [124] illustrated using elastic-plastic finite element simulation results that the local stress concentration at pores can induce fatigue cracks. Smith et al. [125-126] performed studies on different notch root radii showing that fatigue life is directly related to the size of notches. Although these experimental studies included external notches, clearly the significance to multiscale modeling was that the notches could be internal or external to induce fatigue cracks. It was the works of Lankford et al. [127-129] that started addressing the difference of length scales related to fatigue crack initiation, small crack propagation, and long crack propagation. Couper et al. [130] and Major [131] experimentally determined that the total fatigue life was directly correlated to the length scale of the pore size in high cycle fatigue of cast aluminum alloys. Davidson et al. [132] and Laz and Hilberry [133] quantified fatigue crack mechanisms from different microstructural features and/or defects. These features confirmed Major's [131] analysis with pores but also included other intermetallics and second phase particles. In an automotive aluminum alloy, Gall et al. [134-136] quantified the effect of particles, intermetallics, and particle clusters. Recently Wang et al. [137] watched via in-situ Scanning Electron Microscopy the growth of a small fatigue crack through a magnesium alloy that showed crack resistance arising from different size scale features: pores, dendrites, grains, and

intermetallics. Kumar and Curtin [138] recently gave a review of various multiscale modeling issues and experiments related to fatigue cracks and the associated microstructure that affects crack growth.

In terms of cyclic plasticity, Shenoy et al. [139,140], Wang et al. [137], and McDowell [141] performed hierarchical multiscale modeling of Ni-based superalloys employing internal state variable theory. Fan et al. [142] performed a hierarchical multiscale modeling strategy for three length scales.

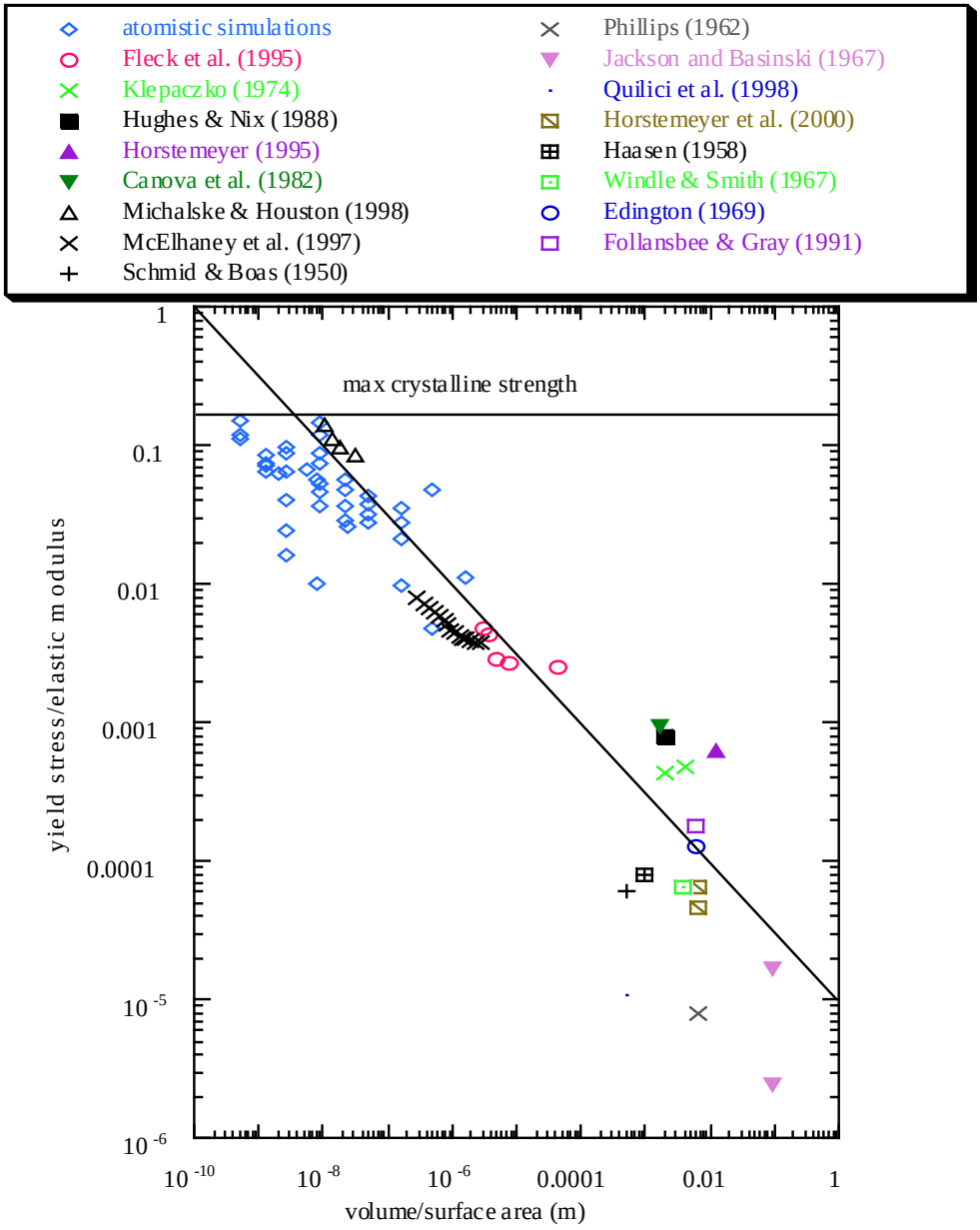

Fig. 4. Yield stress normalized by the elastic shear modulus plotted against a size scale parameter (volume per surface area) illustrating the six orders of magnitude of stress levels and ten orders of magnitude of size related to plastic behavior of single crystal metals [152].

In more recent years since the advent of parallel computing, computational materials science has revealed some various length scale dependencies on yield and plasticity as well. Horstemeyer et al. [64,143,144-151] found that the yield stress is a function of the volume-per-surface-area length scale parameter that correlates well with dislocation nucleation. Figure 4 illustrates that for any kind of size scale experiment related to volume-per-surface-area or fundamental simulation capability where dislocation nucleation is critical, a clear relationship arises [152]. Potirniche et al. [118] showed at the atomic scale through molecular dynamics that void growth and coalescence showed length scale differences in the elastic region as the specimen size increased, but remained scale invariant in the plasticity regime.

Results from parallel computing have also helped to understand local structure-property relations for fatigue. Fan et al. [153,154] through finite element analysis helped quantify the driving force-resistance of microstructurally small fatigue cracks at pores and defects. Potirniche et al. [119,120] and Johnston et al. [155] employed computational methods to study fatigue crack growth at different length scales: atomic level and crystal level. Gall et al. [156] employed finite element simulations to understand the crack incubation processes that lead to a fatigue crack. After the crack has started but still in the microstructurally small regime, Deshpande et al. [157,158] examined the local plasticity arising from dislocations at a crack tip and the associated fracture growth using a dislocation dynamics theory. Morita and Tsuji [159], Mastorakos and Zbib [160], and Groh et al. [161] used dislocation dynamics theory in a computational setting to understand relationships of plasticity and crack sizes regarding fatigue crack growth.

One can summarize that the materials science multiscale frame of reference, whether it be from experiments or computations, has been a bottom-up approach in trying to find the structure-property relationships. McDowell and Olson [162] gave a comprehensive summary of computational materials with respect to multiscale modeling and an associated educational program. The examples given here are certainly not all-inclusive but at least they are typical of most studies and substantiate the perspective.

3.4 Physics Perspective

At the lowest scales, computational physicists pursued both hierarchical and concurrent methods for joining the electronics principles scale simulations with the atomic scale simulations. Ramasubramaniam and Carter [163] summarized some of the current multiscale methods at the lower scales. In a concurrent manner Lu and Kaxiras [164] and Choly et al. [165] coupled Density Functional Theory (DFT) with the EAM potentials at the atomic scale to analyze different dislocation behavior. Lu et al. [166] extended the original Tadmor et al. [45] quasi-continuum method to couple another length scale by implementing quantum mechanical DFT calculations so that three concurrent domains were represented. To accomplish this Lu et al. [166] needed to include Ercolessi and Adams [167] and Li et al. [168] force matching algorithms for the three disparate length scales. Still others have studied concurrent methods joining quantum models with DFT [169-172].

A different concurrent multiscale method developed within the physics community was termed by the authors as the “learn-on-the-fly” (LOTF) strategy [173]. In this scheme, simple forms of potentials are chosen to represent the interatomic forces. Unlike conventional empirical potentials whose parameters are global and constant, these parameterized potentials in the LOTF scheme are *local* and *variable* and can be changed at run time by means of accessory quantum calculations when deemed necessary. The original potential is assumed to be constructed to accurately describe bulk processes such as the elastic deformation. Hence, most atoms in the system will experience elastic deformation most of the time but when a defect or crack is introduced, the quantum calculations will be invoked. The classical potential “learns”

and adapts to the local environment “on the fly”. The missing information is computed using a “black box” engine based on a DFT or a tight-binding formalism. The dynamic force matching employed here includes the work of Li et al. [168].

Probably the most used hierarchical multiscale method that joined electronics principles simulation results to the atomic level came by means of the EAM or MEAM potentials for metals. The EAM and MEAM have been called “semi-empirical” interatomic potentials, because of their determination in a hierarchical manner. Daw and Baskes [46] were the first to propose a numerical method for calculating atomic energetics (EAM). The major component of EAM is an embedding energy of an atom determined by the lower scale local electron density into which that atom is placed. An embedding energy is associated with placing an atom in that electron environment to represent the many-body effect of the neighbors. The formalism is nonlocal in nature and hence because of the many-body interactions, metal responses could be realized. Daw et al. [47] reviewed the basic method and several applications of EAM. The MEAM potential, later proposed by Baskes *et al*. [174-177], was the first semi-empirical atomic potential using a single formalism for fcc, bcc, hcp, diamond-structured materials and even gaseous elements, and produced good agreement with experiments or first principles calculations. The MEAM extended EAM to include angular forces similarly in the solid mechanics sense of bending of an Euler Beam to a Timoshenko Beam.

The EAM and MEAM potentials once determined from electronics principles calculations [178] have been used to reproduce physical properties of many metals, defects, and impurities. For example, EAM molecular statics, molecular dynamics, and Monte Carlo simulations were performed on hydrogen embrittlement effects on dislocation motion and plasticity [46,179-181]. These potentials have been used to analyze plasticity [74,144,145,148-150,182,183], cracks and fracture [117,184], and fatigue [119,120,185,186].

3.5 Mathematics Perspective

Although mathematics plays a major role in all of the previous perspectives (solid mechanics, numerical methods, materials science, and physics) there are aspects of the math perspective that purely start from mathematical concepts. Brandt [187] and Weinan and Engquist [188] have suggested various mathematical paradigms to address multiscale modeling. The previously discussed perspectives essentially use mathematics as a means to an end. It is worth mentioning that certain mathematical formulations have been developed for multiscale modeling, from a purely mathematical perspective. Some of the perspectives include dimensional analysis, fractal and self-similarity analysis, Percolation theory, and statistical design of experiments.

A good example of starting from a mathematical perspective is the work of Barenblatt [189], who, using dimensional analysis and physical self-similarity arguments, described the art of scaling relationships. He demonstrated the concepts of intermediate asymptotes and the renormalization group as natural consequences of self-similarity and showed how and when these tools could be used for different length scale analyses. In comparing dimensional analysis and renormalization group theory Carpinteri et al. [190] examined the ductile to brittle transition in metals in which by increasing the structural size the tensile strength and fracture energy changed. In another dimensional analysis study, Cheng and Cheng [191] employed dimensional analysis with finite element simulations to quantify the size scale relationship with conical indentation of elastic-plastic work hardening behavior. Using asymptotic expansions, Ansini et al. [192] employed a nonlocal functional to capture behavior for a multiscale analysis and applied this analysis concept to a nonlinear elastic spherical shell.

Self-similarity is a mathematical concept in which fractals have been applied to predict or simulate some solid material behavior. A fractal is generally "a rough or fragmented geometric shape that can be spilt into parts, each of which is (at least approximately) a reduced-size copy of the whole," [193]. A fractal typically has a coarse structure with a subscale fine structure that is approximately similar to the course structure. It is typically irregular having a Hausdorff dimension greater than its topological dimension. Long before Mandelbrot thought about fractals, the notion of self-similarity and the associated mathematics began in the 17th century when Leibniz considered recursive self-similarity. In Mandelbrot [194], the fracture surfaces of metals were argued to have fractal characteristics. In the same year Mark and Aronson [195] suggested that fractals can be related to brittle fracture surfaces of rocks. Several years later, Chelidze and Guguen [196] found experimental evidences of fractal type fractures in different rock types. Mosolov et al. [197] then extended the application of fractal geometries to other brittle materials that fractured as a result of compressive loads.

In using differential self-similarity concepts Dyskin [198] determined the effective characteristics and associated stress concentrations of pores, cracks, and rigid inclusions. He proposed a sequence of continua at increasing size scales with each representative volume element determined by an associated microstructure. Power laws with exponents representing the scaling of the microstructure and are not necessarily tied to the material fractal dimension. This formalism was based upon the earlier microstructurally-based representative volume element definition by Graham and Yang [199] and Lee and Rao [200], who discussed the pertinence of enlarging the size of an RVE because of the multitude of different microstructural features that require admission into an RVE. To numerically address these issues of length of the RVE with respect to the microstructures and their associated gradients and subsequent effects on the periodicity assumption, Fish and Wagiman [201], Fish and Yuan [202], and Nuggehally et al. [203] proposed enhancements to the homogenized solutions.

Contrary to self-similar concepts, He et al. [204] and Wang et al. [205] argued that once fracture occurs at a certain scale the discontinuity invalidates any self-similar notion. In other words, the fracture introduces a singularity within the self-similar material at that scale. A scale lower would then not be self-similar.

Percolation theory has been another mathematical tool to address scaling issues. One of the earliest works on percolation theory related to size scale effects was that of Essam [206] who linked clusters of entities with different correlation functions. Greenspoon [207] employed an asymptotic analysis with a scaling parameter that quantified correlation lengths. Later Kestin [208] presented an overview of percolation theory applications to different size scale issues. Percolation Theory has been used for different multiscale aspects of materials. Otsubo [209] used percolation theory to determine particle sizes in suspensions of polymer systems. Leclerc and Olson [210] proposed a percolation model for lignin degradation such that low values for the cluster size exponent obtained during wood degradation were in agreement with diffusion aggregation processes. In a different application, Fu et al. [211] employed a percolation model to describe porosity distributions in a ceramic. Ostoja-Starzewski [212] combined a self-consistent method with a percolation model to describe size effects of an inelastic material with random granular microstructure. In particular, the author found a decrease in scatter in strength with a decrease in specimen size.

In terms of different scale bridging, statistical methods can play a key role in determining which particular subscale features are most important. Bai et al [213] gave a nice review of using statistical methods for multiscale modeling. Another example that summarizes statistical methods bridging many length scales was that discussed by Reichl [214]. However, the key is to determine the appropriate microstructural characteristic related to the pertinent statistics. For example, a dilemma might arise as the size of the representative volume element needs to be

large enough to capture the statistics of the represented microstructures and defects but must be small enough to represent a continuum element in finite element analysis. As discussed earlier, materials scientists may assert that dendrite cell size is a predominant feature on the fatigue life of a cast specimen, because they perform structure-property experiments to quantify the effect. Even though there may be a direct correlation between the size scale feature called dendrite cell size and fatigue life, dendrite cell size may not be the cause of the fatigue failure. For example, as a casting solidifies, the dendrites push the porosity arising from hydrogen within the melt. As such, the dendrite cell size correlates with the porosity and scales with the pore size. Major [131], Zhang et al. [215], Horstemeyer et al. [147], and Horstemeyer and Wang [216] showed that it was the pore size and associated statistics related to pore nearest neighbor distance and pore volume fraction that were the critical cause-effect parameters related to fatigue life and not the dendrite cell size. However, it took experiments and statistical methods coupled with finite element analysis to help determine this relationship for a hierarchical multiscale method for fatigue.

In statistics, ANalysis Of VAriance (ANOVA) is a collection of statistical models, and their associated procedures, in which the observed variance is partitioned into components due to different explanatory variables. The initial techniques of the analysis of variance were developed by the statistician and geneticist R.A. Fisher in the 1920s and 1930s, and is sometimes known as Fisher's ANOVA or Fisher's analysis of variance, due to the use of Fisher's F-distribution as part of the test of statistical significance.

These techniques by Fisher [217,218] can help to sort out the parametric effects efficient and clear of a multiscale analysis. The Design of Experiments (DOE) approach, popularized by Taguchi [219,220] in the field of quality engineering, has recently been utilized in various contexts of mechanics problems and design by Horstemeyer and Gokhale [221], and Horstemeyer and Ramaswamy [115], and Horstemeyer et al. [222]. The DOE methodology enables an investigator to select levels for each subscale parameter and then conduct numerical experiments in order to evaluate the effect of each parameter in an efficient manner. Any number of parameters and levels for each parameter can be placed in an orthogonal array, which lends itself to optimal determination of parametric effects. Here, orthogonality refers to the requirement that the parameters be statistically independent. The basic terminology of orthogonal arrays $L_a(b^c)$ is as follows: a denotes the number of calculations, b denotes the number of levels for each parameter and c denotes the number of parameters. As such many parameters can be evaluated with others at that particular scale and the most influential ones can be determined to be used for the next higher scale analysis.

4. Multiscale Modeling of Different Materials

The recent growth of multiscale modeling has permeated every material type known to mankind regarding structural members. Although most of the work has been focused on metal alloys, because they have been used the most over time as reliable structural materials, multiscale modeling has also been employed for ceramics and polymer systems (both synthetic and biological).

4.1 Metals

Since most of the methods and examples in this review are focused on metals, this section will be shortened. Albeit, it is important to note that multiscale modeling has been applied to basic metal alloy structures: face center cubic aluminum alloys, hexagonal close pack magnesium alloys, and body center cubic iron and steel based alloys.

4.2 Ceramics

The least of amount of multiscale modeling has probably been performed on ceramic materials, basically because they are the least used material system for structural applications, especially when large ductilities are required. Furthermore, since ceramics are essentially linear elastic, the need for multiscale modeling has not been warranted. However, some multiscale studies have certainly been performed on these materials. For example, Mauro and Varshneya [223,224] performed multiscale modeling studies on various glass structures comprised of different ceramics. Krishnamurthy et al. [225] developed a multiscale model for zirconia in which they studied oxygen diffusion. Hansen et al. [226], Schmittbuhl et al. [227] and Hansen and Schmittbuhl [228] employed multiscale modeling for brittle cracks focusing on surface roughness and related it to percolation theory.

4.3 Polymers

The use of multiscale modeling for polymers and polymer-based systems can be distinguished into synthetic (man-made) and biological (God-made) materials. Although synthetic polymers have been used as monolithic structural materials, like polyurethane, polypropylene, and rubber, probably the broadest usage for structural applications is in composites of some type in which short or long fibers that have high tensile strength are found. A further breakdown of biological materials can be divided into human and animal materials and vegetation. A discussion of multiscale modeling opportunities with biological materials was presented by Chong and Ray [229].

4.3.1 Monolithic Synthetic Polymer Multiscale Modeling

Multiscale polymers, in the absence of strengthening or stiffening material, have multiscale structure depending on the volume fractions of crystalline and/or amorphous segments. For example, Theodurou [230] also performed a hierarchical multiscale analysis on amorphous polymers. Another multiscale study was that of Ismail et al. [231] who performed a hierarchical averaging scheme using wavelet transforms to study multiscale behavior of polymers. An example of the multiscale methodologies moving into the industrial sector is that of Bicerano et al. [232], who described their hierarchical multiscale modeling methodologies at The Dow Chemical Company. Yu and Fish [233] developed a multiscale, multiphysics concurrent method for analyzing viscoelastic behavior using asymptotic analysis to capture the spatially varying important length scales. Finally, Curgul et al. [234] performed MD simulations of amorphous polymer nanofibers (1.9 to 23.0 nm) to study their size-dependent properties. The fibers comprised chains that mimic polyethylene, with chain lengths ranging between 50 and 300 carbons. The result was that the glass transition temperature of these amorphous nanofibers decreased with a decreasing fiber diameter.

4.3.2 Composite Synthetic Polymer Multiscale Modeling

Next to metals, probably the synthetic polymer-based composites have been modeled most by hierarchical multiscale methods. Different multiscale formulations have been approached: top-down internal state variable approaches, self-consistent (or homogenization) theories, and nanoscale quantum-molecular scale methods.

Probably the earliest works of trying to model different length scales of damage in composites was that of Halpin [235,236] and Hahn and Tsai [237]. In these models they tried to deal with polymer cracking, fiber breakage, and interface debonding between the fiber and polymer matrix, and delamination between ply layers. Each of these different failure modes were represented by a length scale failure criterion formulated within a continuum. As such, this

was an early form of a hierarchical multiscale method. Later, Halpin and Kardos [238] described the relations of the Halpin-Tsai equations with that of self-consistent methods and the micromechanics of Hill [29].

The Halpin-Tsai equations were based upon purely mechanics arguments from micromechanics. It was not until Talreja [14-16], Chang and Allen [239], Allen [240], Costanzo et al [241] and Krajcinovic [242-244] that thermodynamics of appropriate internal state variables for damage in composites under mechanical loads were addressed. Similar to the metal plasticity theoreticians, these researchers employed Coleman and Gurtin's [11] thermodynamic framework to determine the kinetic equations. However, unlike the metal internal state variable community that could quantify the evolution equations for dislocations and damage, these polymer-based composites theoreticians did not propose evolutionary rate equations, just damage state equations.

In terms of numerical procedures for multiscale modeling, Fish and Shek [245] laid out a numerical technique for global and local interactions for composites. Later, Fish and Yu [246] in a three-scale concurrent multiscale methodology for composites analysis introduced a nonlocal damage model.

Different studies using homogenization theory have been performed on composites structures. One such example was that Belsky et al. [247] who presented a multiscale modeling method that included critical deformation modes, vibration and buckling modes, and failure modes (delamination, debonding, and microbuckling). Hassani and Hinton [248-250] published a set of papers focusing on the analytical and numerical methods for the theory of homogenization and optimization. They showed that the methods can be used for topological features such as geometries and microstructures to bridge two different length scales. Lourenco et al. [251] recently reviewed the multiscale aspects of masonry structures, which are really polymer based composites, using homogenization theory. Matous et al. [252] recently performed a multiscale analysis on hetereogeneous thin layers using homogenization theory for cohesive failure.

Aboudi [253,254] and Paley and Aboudi [255] developed various micromechanical finite element simulations at the mesoscale with the "Generalized Method of Cells." More recently, Williams and Tippetts [256] reviewed multiscale modeling approaches for polymer-based composites and proposed a model of their own. Their hierarchical multiscale model comprised three size scales. The macroscale was associated with the plate thickness and a mesoscale associated with the lamina thickness. The mesoscale focused on lamina and ply splitting processes using a cohesive zone model with adaptive meshing. The lowest length scale corresponded to a material point within each lamina and was modeled by a new stochastic homogenization theory.

With the advent of nanomaterials, different types of polymer-based composites arose as multiple scale analysis down to the nanoscale became a trend for development of new materials with new properties. Multiscale materials modeling continue to play a role in these endeavors as well. For example, Qian et al. [257] developed multiscale, multiphysics numerical tools to address simulations of carbon nanotubes and their associated effects in composites including the mechanical properties of Young's modulus, bending stiffness, buckling, and strength. Maiti [258] also used multiscale modeling of carbon nanotubes for microelectronics applications. Friesecke and James [259] developed a concurrent numerical scheme to evaluate nanotubes and nanorods in a continuum.

Wescott et al [260] in a hierarchical sense used atomistic simulations, mesoscale simulations, and finite elements to examine the effect of nanotubes that were dispersed in

polymers. This bottom-up multiscale method employed percolation notions in trying to bridge the effects of the subscale nanotubes.

4.3.3 Human and Animal Multiscale Modeling

The human body is a very complicated machine differentiating itself from non-living matter. The added "living" and thus changing with higher frequency than the metal, ceramic, and synthetic polymers that we have discussed makes multiscale modeling more difficult. Combine this with the fact that the human has very different organ structures makes modeling the human (or any animal for that matter) even more complex. Even with these complexities, researchers have tried to distinguish the multiscale effects of the different organs.

For the vascular system, Lagana et al. [261] employed a hierarchical methodology for multiscale modeling of pulmonary and coronary perfusions in the cardiovascular system. Essentially, they studied different shunt size effect on the pressure of blood within the vessels.

For bone, several studies have been performed. Ho Ba Tho et al. [262] and Budyn and Hoc [263] studied human cortical bone with a multiscale modeling focus on aging and fracture. Fritsch and Hellmich [264] performed micromechanics simulations analyzing different microstructural patterns in bone thus quantifying the anisotropic effects. For trabecular and cortical bone, Porter [265] employed a hierarchical multiscale modeling methodology by using a hybrid nanocomposite paradigm to analyze bone. Of course, bone is attached to other tissue, so the various length scales related to these attachments can be an issue in modeling the human body. Katz et al. [266] performed a hierarchical multiscale characterization in order to quantify the structure-property relations for multiscale modeling of calcified tissues at the bone-tissue interface. For cartilage, the multiscale modeling has been limited to homogenization models [267]. Hellmich et al. [268] argued through multiscale modeling that trabecular bone and cortical bone have fundamentally the same materials although a different structural morphology. They argued that both types of bone comprise hydroxyapatite, collagen, ultrastructural water, non-collagenous organic materials, and marrow with water filling the Haversian canals. Homogenization theory was used to model the different scales of analysis. Taylor [269] reviewed the strength and fracture toughness of bone from a multiscale perspective. In this review, Taylor [269] not only discussed the morphology effects at each length scale but the density variations and the ability to adapt its living structure as well. Kawagai et al. [270] in a multiple scale analysis that incorporated x-ray computed tomography quantified at different length scales the apatite crystallite orientation (texture) related to the stress state in that continuum point. A homogenization method was used to bridge the scales. Clearly anisotropic behavior was quantified arising from the crystallite orientation.

The brain has briefly been examined from a multiscale perspective. Imielinska et al. [271] in order to determine trauma injury to the brain under a ballistic impact or blast to the head developed a multiscale high fidelity biomechanical and physiologically-based modeling tools. They employed their methodology on pigs, so understanding of the human brain is still lacking.

To generalize the human body, Bassingthwaithte et al. [272] purported a multiscale modeling strategy for cell-to-organ systems. They employed self-consistent models at each scale to represent RVEs related to biophysical and biochemical rate of changes (protein, cells, tissues, and organs). For example, for a protein representation at a continuum level, the subscale information focused on gene signaling and regulation of transcription and translation.

4.3.4 Multiscale Modeling of Vegetation-Based Structural Materials

In terms of multiscale modeling for vegetation, there have been only a few studies. Silva [273] suggested a hierarchical method for analyzing naturally occurring bamboo for use in synthetic man-made structures. Since naturally occurring bamboo has complicated multiscale

internal structures at different length scales, a homogenization model to represent the mechanical behavior was introduced. The homogenization included a functionally graded representation in a finite element analysis domain. Godin and Caraglio discuss and present a model for the different topological length and time scale structures within trees. Their model supports multiscale, attributed and time-varying descriptions of trees intended to be used for plant analysis methodologies and plant growth simulations. Makela [274] presented a hierarchical multiscale model to address the dynamic growth of trees. In particular the author included modeling for patterns as well as size growth. The motive was trying to quantify wood quality.

5. Multiscale Modeling for Design

A significant opportunity exists for multiscale modeling in the next wave of design paradigms for components, subsystems, or large scale systems by accounting for the structure-property relations which have a real impact on measured system response to design loads. As multiscale modeling is refined and enhanced the degree of model accuracy and precision is directly related to the level of product design optimization which can be achieved. When combining multiscale modeling into simulation-based design concepts, several challenges include: lack of validated techniques for bridging the various time and length scales, management of models with the associated uncertainties, management of a huge amount and variety of information, and development of simpler, user-friendly methods for efficient decision making.

Panchal et al. [275] discussed how multiscale modeling deals with efficient integration of information from multiscale models to gain a holistic understanding of the system, whereas multiscale design deals with efficient utilization of information to satisfy design objectives. In order to address the challenges associated with multiscale design, Panchal et al. [275] proposed a domain independent strategy based on generic interaction patterns between multiscale models.

In a different vein, Olson [86,87,276] has described the processing-structure-performance relationship as a function of multiscale, multilevel materials attributes that has lent itself to multiscale modeling and simulation. In the DARPA AIM project [277] a Ni-Base superalloy employing a hierarchical multiscale method was used to design a component in a gas turbine engine with the objective of increasing burst speed and decreasing the disk weight. The focus on materials design was exemplified in Olson [278] in which martensite was examined through a multiscale method.

In joining the Olson and Panchal et al. strategies, the Mistree [279] research group at Georgia Tech has focused on using hierarchical multiscale modeling to optimize materials design. The classical materials selection approach is being replaced by the *design* of material structure and processing paths based on a hierarchy of length scales for multifunctional performance requirements. In Seepersad et al. [280,281] they optimized the mechanical properties for cellular foam with voids.

6. Multiscale Modeling in Manufacturing

Besides design, another great opportunity for multiscale modeling is the venue of materials processing. Rapid prototyping and other materials processing techniques can facilitate tailoring microstructural topology with high levels of detail. This industrial framework makes it amenable for multiscale materials modeling to affect a paradigm shift with US manufacturing. Economists Grimes and Glazer of the Examination Bureau of Labor Statistics stated that the US has lost 18% of its manufacturing jobs from 1990 to 2003. Although higher labor costs in the US are a big factor, US industry has lacked improvements in innovative design. An upturn in

the manufacturing industry clearly requires a competitive advantage through better design tools based on information technology and high-fidelity multiscale materials modeling and simulations and design optimization. Horstemeyer and Wang [216] argued that improved design/analysis capabilities based on recent scientific and engineering research advances will provide a substantial benefit to the US manufacturing industry, but to do so multiscale modeling is needed in the mix. This applies to the general manufacturing industry, specific "made-to-order" manufacturing segments, and those involved with cutting edge technologies. Significant breakthroughs in the knowledge base, software integration, length/time scale bridging, and educational enterprise are required to reverse the negative manufacturing trend in the US. Right now multiscale modeling can be used to optimize the process-property-cost for processes such as forging, forming, casting, extrusion, rolling, stamping, and welding/joining.

7. Engineering Designs in Practice using Multiscale Modeling

Two different metal alloy examples using multiscale modeling will next be shown to illustrate the integration of many disciplines described earlier. One example of optimizing an aluminum alloy based automotive control arm for a Cadillac automobile demonstrates multiscale modeling of plasticity and damage/failure in a hierarchical manner. Another example of employing multiscale modeling will be shown by optimizing a magnesium alloy with respect to fatigue that was used to redesign a Corvette cradle, which is the main structural undercarriage under the engine. These hierarchical multiscale modeling examples incorporate solid mechanics, mathematics, materials science, and physics with various bridging methodologies.

7.1 Plasticity-Damage Multiscale Modeling Example of Automotive Cadillac Control Arm Design

In designing a structural component, a failure analysis will typically include a finite element analysis and microstructural evaluation. Sometimes the microstructural evaluation will quantify the inclusion content (source of damage in a component) in a prioritized fashion differently than the finite element analysis. Let us consider the hypothetical situation exemplified in Figure 5. Here we have an automotive control arm that has undergone certain boundary conditions in a finite element analysis. The finite element analysis with homogeneous microstructural considerations revealed that the highest Von Mises stress [282] occurred at Point D. On the other hand, microstructural analysis using optical imaging revealed that the largest defect occurred at Point B. Both the finite element analysis and microstructural analysis camps would argue about the location of final failure. However, in our example, both are wrong, because the final failure state is both a function of the initial inclusion state and the boundary conditions. As such, Point A failed first. The key now is the development of a tool that captures Point A failing first [146]. The effective solution to this structural dynamic analysis/design problem is the development of a hierarchical multiscale modeling methodology that admits the appropriate structure-property relations from each length scale so that proper hetereogeneous microstructures can be included in a finite element analysis.

The fundamental difficulty in quantifying the structure-property relations arises because of the different length scales of microstructures and defects present within a material. The challenge of developing a mathematical representation of these different length scale features and their associated evolution into various damage states is great. However, this lends itself to a hierarchical multiscale methodology in which multiple space scales and associated non-equilibrium evolution damage evolution need to be quantified.

In order to start the multiscale modeling, internal state variables were adopted to reflect void/crack nucleation, void growth, and void coalescence from the casting microstructural

features (porosity and particles) under different temperatures, strain rates, and deformation paths [115,116,221,283]. Furthermore, internal state variables were used to reflect the dislocation density evolution that affects the work hardening rate and thus stress state under different temperatures and strain rates [25,283-285]. In order to determine the pertinent effects of the microstructural features to be admitted into the internal state variable theory, several different length scale analyses were performed. Once the pertinent microstructural features were determined and included in the macroscale internal state variable model, notch tests [216,286] and control arm tests were performed to validate the model's precision. After the validation process, optimization studies were performed to reduce the weight of the control arm [287-289].

Stress (from highest to lowest)	Inclusion (from most severe to less severe)	Damage (from most severe to less severe)
D	B	A
A	E	D
C	A	E
E	D	C
B	C	B

Fig. 5. Stress and inclusion analysis studies can be independently performed on this control arm, but both would give an erroneous location of failure, because damage accumulation is dependent upon both entities.

In order to quantify the structure-property relations at each scale, a multiscale hierarchy of numerical simulations was performed coupled with experiments to determine the internal state variable equations of macroscale plasticity and damage progression as illustrated in Figure 6. The microstructures/defects observed in the cast A356 aluminum alloy in descending order of deleterious effect were found to be large oxides/pores, smaller oxides/pores, silicon particles, dendrite cells size, and intermetallics. The attributes of these features that were included in the model were the size distributions, volume fractions, and nearest neighbor distances.

Now that the top-down internal state variable theory was established, the bottom-up simulations and experiments were required. At the atomic scale (nanometers), simulations were performed using Modified Embedded Atom Method (MEAM) Baskes, [176] potentials based upon interfacial atomistics of Baskes et al. [177] to determine the conditions when silicon fracture would occur versus silicon-interface debonding [156]. Atomistic simulations showed that a material with a pristine interface, would incur interface debonding before silicon fracture. However, if a sufficient number of defects were present within the silicon, it would fracture before the interface would debond. Microstructural analysis of larger scale interrupted strain

tests under tension revealed that both silicon fracture and debonding of the silicon-aluminum interface in the eutectic region would occur [290-291].

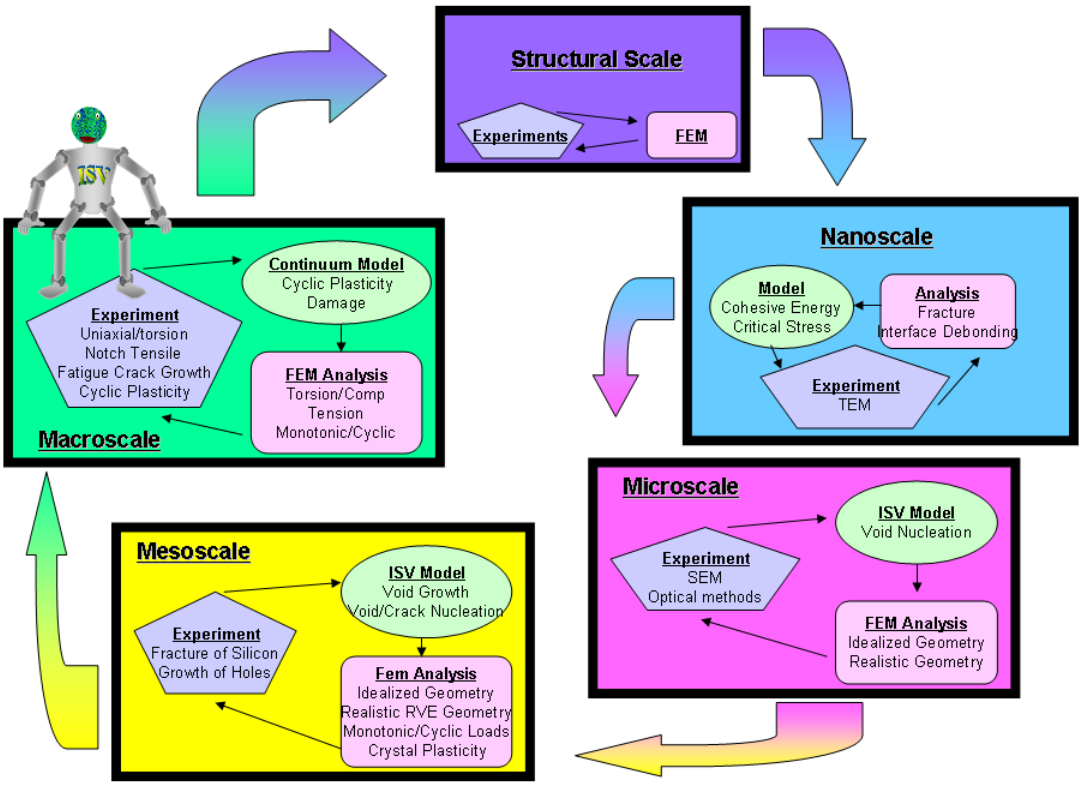

Fig. 6. Schematic illustrating the corroboration of multiscale modeling and multiscale experiments at each length scale and the pertinent effects being pushed up to the next higher length scale.

Another important result from the atomistic simulations was that the stress-strain response of a region of material around an interface that debonded could be represented by an elastic fracture analysis at the next higher size scale if the interface were assumed to be larger than 40 Å. Hence, an elastic fracture criterion was used in the microscale (1-20 microns) finite element analysis, which focused on void-crack nucleation and mesoscale (1-200 micron) finite element analyses, which focused on silicon-pore coalescence [216].

The micron size scale finite element analyses focused on the void-crack nucleation progression by examining the parameters that influenced silicon fracture and silicon-aluminum interface debonding [216]. In particular, we included temperature, shape, size, nearest neighbor distance, number density, prestrain history, and loading direction as parameters for the silicon in the finite element analyses. The parametric study employing an ANOVA design of experiments method clearly showed that the temperature dependence on void nucleation from silicon fracture and interface debonding was the most dominant influence parameter. To verify this result, we performed notch tensile tests at ambient temperature and the two extreme limits of temperatures that a control arm would experience: 222 K and 600 K [288]. From examining the fracture surfaces and cross-sections of deformed samples and counting the number of void nucleation sites, it was clear that at the coldest temperature, the largest voids nucleated and at the hottest temperature, the least amount of voids nucleated. Essentially, the colder temperatures induced a higher local stress state. The higher stresses fuse damage at an increased rate. These

results corroborated the microscale finite element analyses and thus a temperature dependence on the void nucleation rate was included in the macroscale ISV model. As a follow-on, strain rate tests were also performed in which the strain rate effect on void nucleation was quantified for the model [289].

An important set of experiments was performed to determine the void nucleation rate under different stress states and strain levels [287]. Interrupted equivalent strain test specimens that underwent tension, compression, and torsion were examined via optical imaging and the number densities of fractured/debonded particles were quantified. The experimental data showed that the void nucleation rate under torsion was the highest followed by tension and then by compression. Interestingly, the highest work hardening rate was exhibited in compression followed by tension and then by torsion. This inverse relationship of the work hardening rate to the void nucleation rate revealed a coupling between the stress state and damage progression. The void nucleation rate and work hardening rate differences were included in the macroscale void nucleation internal state variable model.

In the Mesoscale I analyses (1-200 microns), the simulations focused on pores arising from silicon fracture and interface debonding that interacted with pores from the casting process. In performing these finite element analyses, the finite element meshes were constructed on real A356 micrographs. Hence, the sizes, distributions, and volume fractions of silicon, casting porosity, and dendrite cells were inherently imbedded in the simulations. Indenter tests were conducted on the particular second phases to determine the elastic moduli of the silicon, intermetallics, and matrix aluminum. Compression tests were also conducted on the eutectic aluminum at different temperatures to obtain the stress-strain responses for the mesoscale analyses. These values were used for the finite element simulations. The progression of silicon fracture and interface debonding were matched from the interrupted strain experiments described earlier by a trial-and-error method for the local elastic fracture silicon stresses. The applied stress state was then varied with the temperature, and strain rate. The results gave insight into the functional form of the equation needed for the macroscale coalescence equation [292]. Furthermore, temperature dependence was deemed as very important here. In fact, the influence of temperature on void coalescence was the opposite trend as that of void nucleation. For void nucleation, as the temperature decreased (increasing the stress level), the void nucleation rate increased. For void coalescence, as the temperature increased (increasing the plastic strain), the void coalescence rate increased. This temperature dependence was included in the macroscale coalescence equation.

The Mesoscale II finite element simulations (100-500 microns), focused on pore-pore interactions to give insight into coalescence from casting porosity. Similar to the void nucleation parametric study, an ANOVA design of experiments method was used by varying temperature, shape, size, nearest neighbor distance, number density, prestrain history, and loading direction and monitoring the total void growth and strain at localization [115]. The results showed that temperature, again, was a first order influence parameter on void coalescence because it increases the local plastic strains, but the size of pore and type of loading (triaxial state of stress) were first order influence parameters on strain localization. Furthermore, microporosity, prestrain history, and number density were first order influences, along with temperature, on the total void growth. Hence, these attributes were placed in the macroscale coalescence equation. The macroscale void growth and coalescence internal state variable equations were then tuned to other micromechanical simulations [116] that were performed to study the evolution rates under varying deformation and temperature.

Another important result from this study showed that if a pore were within eight diameters of another pore, the void growth rates would be enhanced. Alternatively, if a casting can have

nearest neighbor distances of greater than eight pore diameters, then the strain to failure would be increased.

Tension experiments on flat bars were performed to analyze void growth from surface pores under different temperatures (222K, 297K, and 600K). The surface pores were first measured in the virgin state and then the specimens were tested to a certain strain level. The identical voids were then measured again. This process occurred until the specimens fractured. The voids were further than eight diameters apart; hence, the results were used to determine the single void growth equation for the macroscale microstructure-mechanical property model. As it turned out, minimal void growth was measured from these surface pores until the final fracture occurred indicating that void nucleation was probably more important than void growth and coalescence in this cast A356 aluminum alloy under uniaxial monotonic loads. Furthermore, little difference was observed from the temperature changes indicating that macroscale void growth equation did not need to include the temperature dependence.

Given the subscale information, the macroscale total void volume fraction (cm) was a function of the void nucleation rate, void growth rate, and coalescence rate. The coalescence or void interaction rate arose from two sources: pores from silicon fracture and interface debonding interacting with casting pores and two or more casting pores interacting. Once the macroscale equations and the corresponding material constants were determined from the aforementioned analyses, compression tests at different strain rates and temperatures were performed to determine the plasticity parameters [293].

Now that the multiscale modeling and experimentation methodology were completed, several types of macroscale tests (cm) were then performed to validate the methodology. First, cyclic uniaxial tests (Bauschinger effect tests) were performed in which tension was followed by compression and compression was followed by tension up to 2%, 3%, and 5% strain levels [64,294]. Because the work hardening rate was different in compression than tension due to the preferred damage, the stress state at the end of the reverse test was different depending on the path history. Even with this complexity, the internal state variable plasticity-damage model was able to accurately capture this coupling of damage and plasticity. Typical power law plasticity formulations or other formulations that do not have the results of the structure-property relations determined from multiscale modeling would not_capture this phenomenon. The second set of experiments included interrupted notch tests in which the specimens were analyzed nondestructively by x-ray tomography and analyzed via optical imaging analysis [286]. Void volume fractions, sizes, and distributions were quantified at failure, 90% of failure, 95% of failure, and 98% of failure. The finite element analyses, which included the macroscale microstructure-mechanical property model, gave very close results (to within 1%) to the x-ray tomography and optical imaging data.

Once the validation of the physics and verification of numerical implementation was completed, control arm simulations (m) were performed with two goals in mind: first, to finally judge the predictive capability of the model for a control arm, and second, use the model to optimize the control arm by adding mass to certain “weak” regions and taking away mass from “strong” regions. As it turned out, the simulations accurately predicted the final failure locations of the control arm as demonstrated by control arm experiments Figure 7.

The final step in the use of multiscale modeling methodology for this control arm redesign was employing an optimization algorithm to study the reduction of weight potential. A reliability-based optimization was used to integrate the multiscale modeling methodology with the redesign [78]. Although the methodology is generic for any multiscale modeling and redesign situation, the methodology was applied to redesigning a cast automotive control arm. This multiscale modeling example included quantifying uncertainties in the microstructure-

property relationships, the influence of the uncertainties on the plasticity-damage constitutive relationship, and the integration of such models into engineering design of structural components subject to the internal state variable failure criteria. In doing so, a metamodeling approximation was found to be a necessary component of this efficient methodology when considering the noise and nonlinearities in the failure responses. The accuracy and performance of several parametric and non-parametric metamodels were compared to investigate the effect of microstructure-property relations and the associated uncertainties on the optimum design. The results show that a Gaussian representation for the metamodel provided the best response for damage/failure. In the end, control arm weight was reduced approximately 25% of the original weight with an increase in load-bearing capacity of 40%. Clearly, without the multiscale modeling that included the structure-property relations, the exact location and strain level of the failure would not have been realized and the optimization would have been fallible.

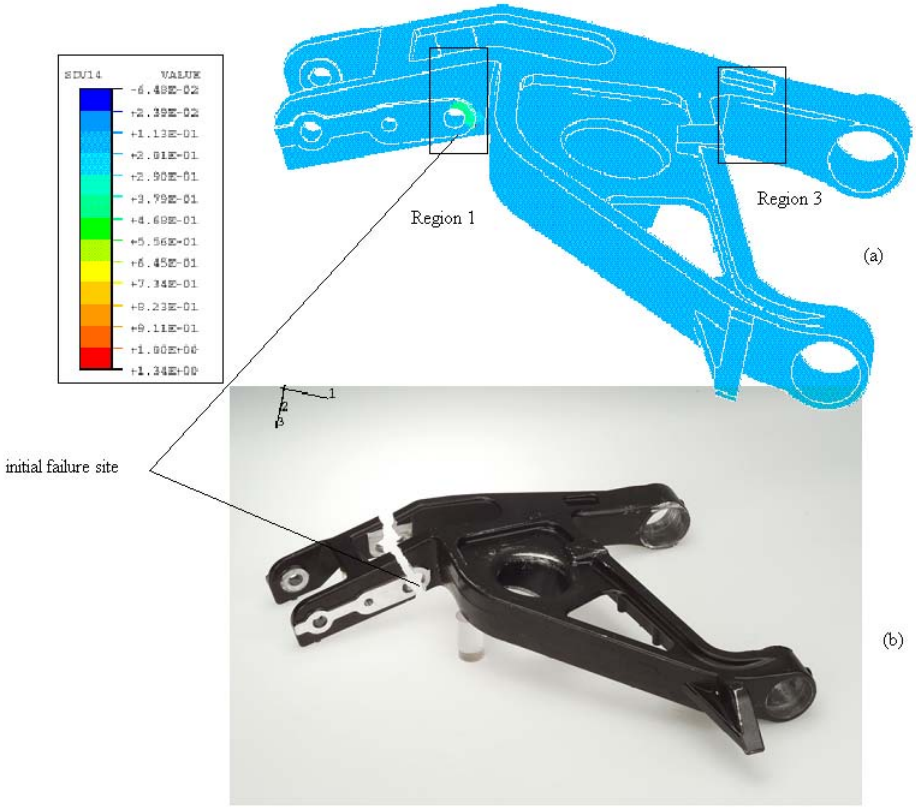

Fig. 7. (a) Control arm simulation result and (b) experimental result comparison showing the failure location. SDV14 is the total void volume fraction or damage level.

7.2 Multiscale Fatigue Modeling Example of Automotive Corvette Cradle

The corvette structural cradle that undergirds the engine and the associated components had been historically made of an aluminum alloy but was being considered to be made of a magnesium alloy. To successfully use a cast magnesium alloy for such an important structural component, it is necessary to understand its resistance to fatigue. In trying to keep reliability with a new material, risk needs to be minimized. Similar to the control arm example the standard method in determining failure locations is to perform a finite element analysis to obtain the highest stresses/strains in a particular region of the material. Some material from that region is then typically extracted and small coupons are made for uniaxial, completely reversed

tension-compression fatigue tests. These results are used to estimate the life of the component. Other material typically adjacent to the coupons is extracted for microstructure/inclusion analysis. Unfortunately, regions that may be important based on the stress analysis may not be important to the microstructural analysis. More importantly, it is the combination of the microstructure/inclusion content with the stress analysis that is needed to determine a precise location for fatigue failure. Therefore, a multiscale modeling effort with multiscale experiments were performed to help redesign and evaluate various magnesium alloys for the cradle.

Figure 8 illustrates the same point as mentioned earlier for the aluminum control arm in that Region D illustratively shows the highest stressed region for this Corvette cradle. The finite element analysis with homogeneous materials characteristics erroneously showed that the failure location to be Point D. Point C showed the most severe initial porosity. Point E actually is where the crack first occurred, so both locations were wrong and Point E realized the combination of the defect state and the boundary value results. This demonstrates again that a clear connection between the microstructure/inclusion content and the mechanical properties are necessary for predicting the life of a structural component.

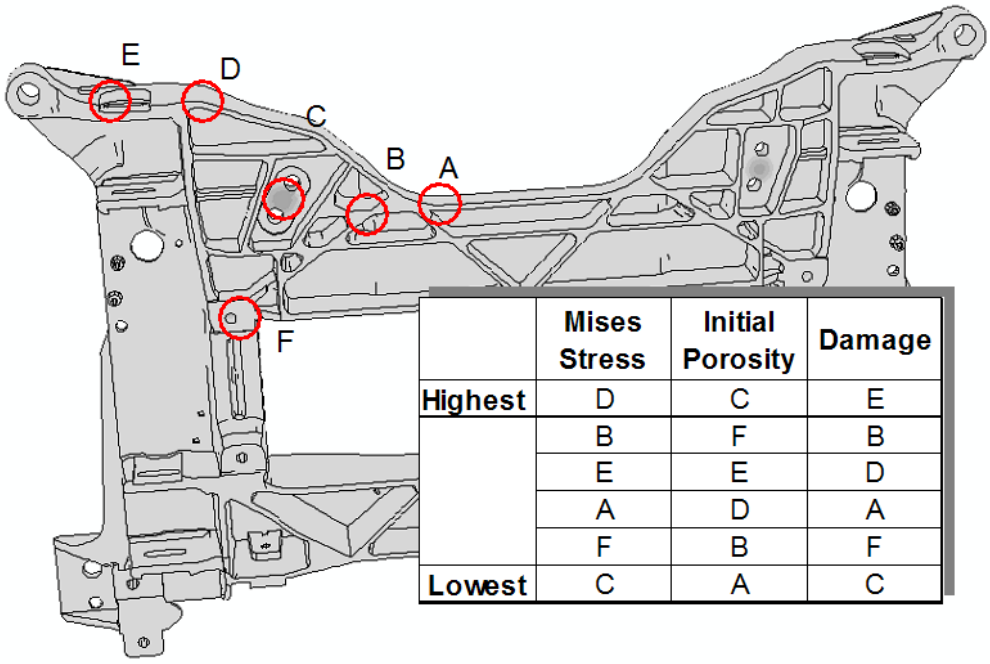

	Mises Stress	Initial Porosity	Damage
Highest	D	C	E
	B	F	B
	E	E	D
	A	D	A
	F	B	F
Lowest	C	A	C

Fig. 8. The highest stress from the finite element analysis was at Point D and the worst inclusion (porosity) was located at Point C. However, the greatest damage from fatigue occurred at Point E, arising from the confluence of the stress state and the initial inclusion condition.

Cast magnesium alloys used for structural applications comprise a highly heterogeneous ductile matrix with several dominant types of inclusions that dictate fatigue resistance. We use the term inclusion as distinctly different from a crack, as the former occur naturally as products of the casting process, while the latter are usually a result of applied loading. The different types of inclusions comprise oxides, gas pores, shrinkage porosity, and distributed intermetallic particles. The matrix usually includes some percentage of aluminum (AM50 has 5% aluminum, AM60 has 6% aluminum, AZ91 has 9% aluminum, and AE44 has 4% aluminum) and is an elastic-plastic material with anisotropic work hardening arising from the hexagonal close pack structure. Large scale oxide films are prone to forming large fatigue cracks that propagate rapidly to premature failure and as such are the most deleterious inclusion. These oxides can range from 200-600 microns. The second most deleterious inclusions are the gas pores. These

gas pores, ranging from 30-500 microns are especially potent in degrading the fatigue resistance as they serve as local stress concentration sites for formation of particularly large cracks that then propagate to premature failure. Another inclusion type operating at a different length scale is the shrinkage porosity that forms by entrapped hydrogen gas in the melt, which grows in concert with the dendrite cell size (secondary dendrite arm spacing) as microstructure coarsens with solidification. Both the gas pores and shrinkage porosity contribute significantly to the localization of cyclic plastic shear strain in the interdendritic regions under fatigue loading. Finally smaller distributed intermetallics on the order of several microns can affect the rate of crack propagation of small fatigue cracks and overall ductility. The most probable casting inclusion to cause fatigue failure was the gas pores as documented for different magnesium alloys [295-297].

The multistage fatigue model of McDowell et al. [298] was originally developed from multiscale modeling for aluminum alloys [299-301] and was applied to these various magnesium alloys for redesign of the Corvette cradle [302]. For each type of inclusion, three different stages exist and each stage incurs a different number of cycles depending on the type of inclusion. Most importantly to recognize is that the different stages represent different length scales of crack lengths. The first stage is the incubation stage, designating pregnancy of the crack. Each type of inclusion incurs a different incubation life with the large oxide being the smallest. No length of crack is assumed here, only the size of the inclusion. The second stage is the Microstructurally Small Crack (MSC) growth regime in which the driving force is governed by the change in the crack tip displacement. In the MSC regime, the resistance from other inclusions in the crack path and the grain orientations and misorientations play a key role. This regime starts at approximately a micron and grows on the order of up to five grain lengths depending on what features are in the crack path. The final regime is the long crack regime, in which Paris Law [303] elastic type behavior takes over with the addition of crack closure coming from the plastic wake [304,305]. We note that for automotive applications 80-90% of the life is spent in the incubation and MSC regimes.

Figure 9 illustrates the multistage fatigue model's calibrated predictions for different types of inclusions illustrating the various length scales involved. Note that the final number of cycles decreases with increasing level of inclusion severity.

To understand the multistage fatigue crack mechanisms for the different inclusion types, multiscale modeling and experiments were performed to develop the top-down model [298]. What the experiments could not provide (even with scanning electron microscopy imaging of the failure surfaces), the micromechanical finite element simulations did [135,136,152,153,306]. Because quantification of the crack incubation and small crack formation stage experimentally was extremely difficult, micromechanical finite element simulations were used to help clarify our understanding of the microstructure-property relations and provide the needed information for the development of the multiscale fatigue model. Since quantification of the local cyclic plastic strain in the microstructure is essential in driving fatigue crack incubation, we focused on that aspect in the micromechanical finite element analyses using both idealized geometries and realistic geometries for the microstructure/inclusion morphology. In particular, we examined the effects of applied stress amplitude, microstructure-inclusion content on the maximum plastic shear strain for crack incubation and the cyclic crack tip opening displacement for MSC crack propagation. For the MSC crack propagation regimes, the effects of particle shape, particle size, particle nearest neighbor dimension, particle distribution, dendrite cell size, pore size, pore shape, pore nearest neighbor distance, and pore distribution were analyzed. In this context such characteristics as crack driving force and crack closure behavior were quantified.

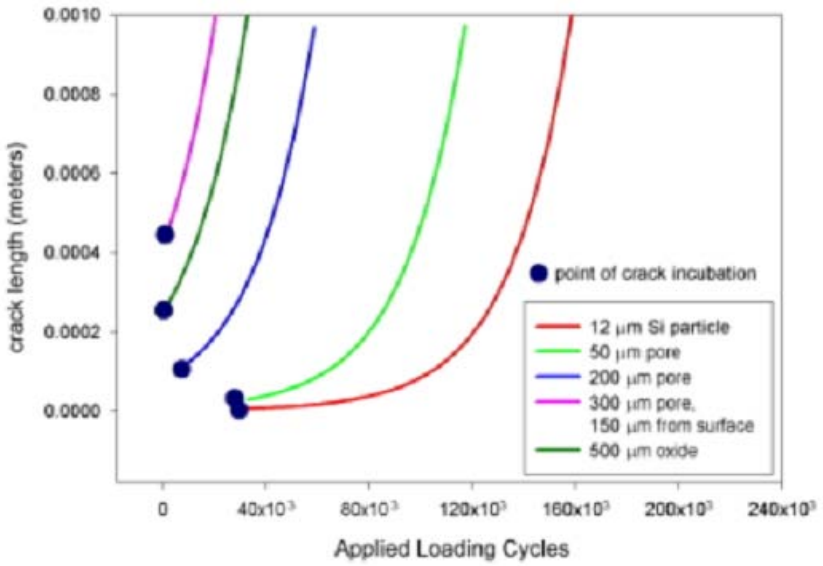

Fig. 9. Multistage fatigue model results illustrating the different length scale inclusions that affect the fatigue life.

For the final magnesium alloy chosen for the Corvette cradle, the multistage fatigue model predicted the mean, upper bound, and lower bound strain-life response for the cast AE44 Mg alloy as shown in Figure 10. To realize the upper bound prediction an inclusion of five microns for a casting pore was assumed with no shrinkage porosity or oxides nearby. For the lower bound a 1 mm diameter casting pore was used. A casting pore mean value of 400 microns was used to yield the mean strain-life curve. As such, the multistage fatigue model gave the designer a notion about not only the mean design for the AE44 mg alloy, but the upper and lower bounds as well. This model coupled with the internal state variable model was then applied to the Corvette cradle.

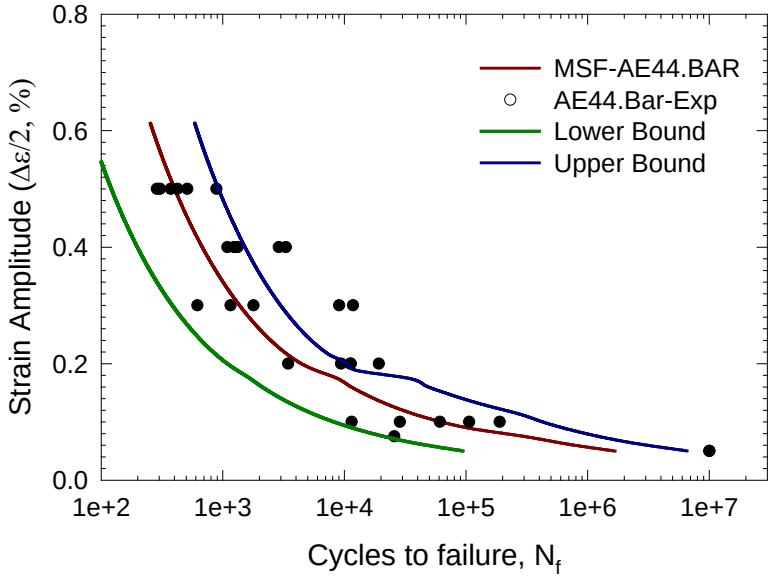

Fig. 10. Uniaxial strain-life experiments and multistage fatigue model predictions for AE44 specimens with predicted upper and lower bounds.

Figure 11 shows that the modeling and simulation results from using the internal state variable plasticity-damage model and the multistage fatigue model gave excellent results when compared to the experimental test results. Once this corroboration was finalized, the models were used to evaluate 35 boundary conditions that a Corvette will experience and verified that the AE44 Mg alloy was a good replacement for the previously cast aluminum alloy.

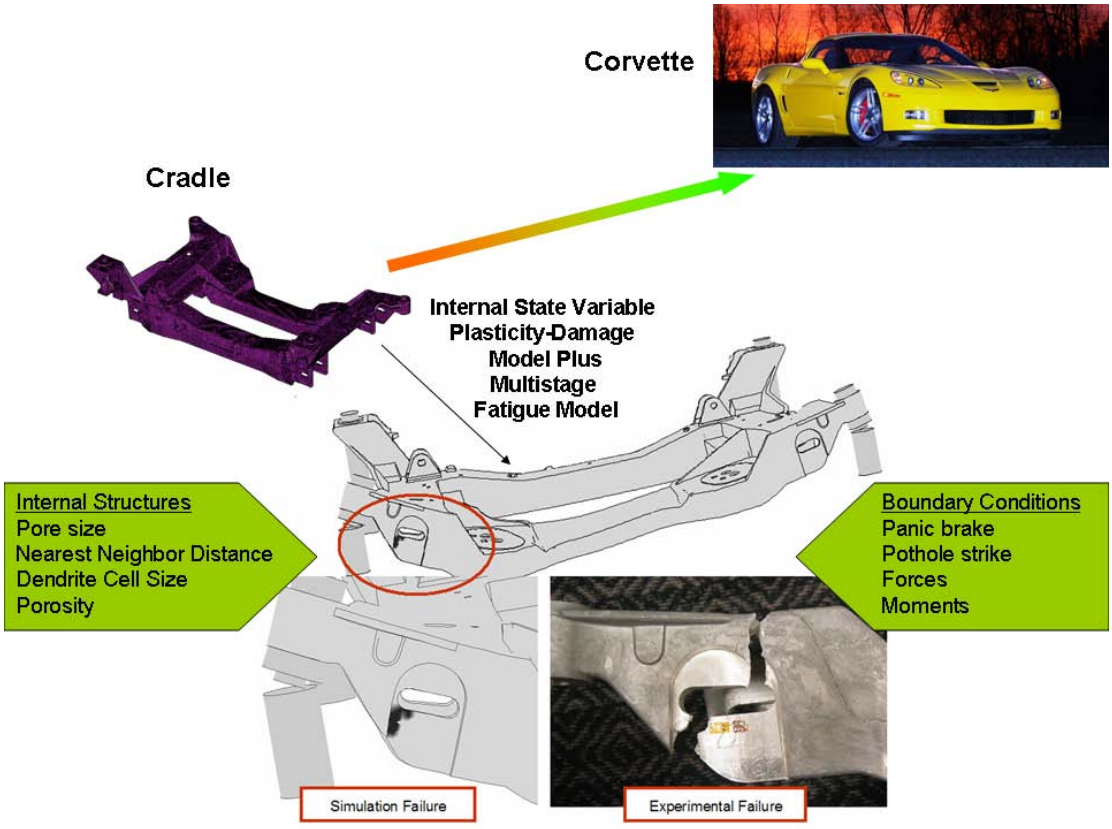

Fig. 11. Corvette cradle modeling and simulation results from the internal state variable plasticity-damage model coupled with the multistage fatigue model demonstrating the capability to predict the experimental result for redesigning the cradle from aluminum to magnesium.

This example of using a hierarchical multiscale modeling methodology for redesign of the Corvette cradle shows that not only can the multiscale modeling be used for monotonic considerations like the control arm, but can be used for fatigue analysis as well.

8. Summary

Glimm and Sharp [307] proposed a challenge to the twenty-first century researcher to consider multiscale materials modeling as a new paradigm in order to realize more accurate predictive capabilities. The context is to predict the macroscale/structural scale behavior without disregarding the important smaller scale features. Multiscale modeling is a key for more accurate simulations for solid materials because of the hetereogeneities arising from these subscale microstructures. As such, the notion of selecting or disregarding the subscale information requires interdisciplinary methods to make proper judgments. When selecting the appropriate subscale feature homogenization, self-consistent methods, percolation theory, etc. are needed to average out the effect within the continuum. As a consequence the terminology

and focus in recent years has helped to gain more accurate component and systems level answers. As demonstrated by several examples multiscale modeling has the capability to ameliorate the better physics versus computational cost conundrum for simulation based design and manufacturing. In the end higher quality more optimized designs are admissible today because of the confluence of computing power, experimental validation techniques, and numerical algorithms available. For multiscale modeling to have even greater impact in manufacturing and design, efficiency even with greater accuracy requires that computational times of the concurrent multiscale methods should be on the order of the computation required for the more accurate treatment using the hierarchical methods. Nothing is really gained from concurrent multiscale methods if this is not true, since hierarchical multiscale methods could be run independently with lesser computational times. This of course, limits the usage of concurrent methods usually to two or three length scales, where hierarchical methods are not limited to just two length scales.

Although multiscale modeling has experienced some success with metals, the usage for polymer material systems has been lacking. In particular, the impact on biological tissue has yet to be realized. Furthermore, the common usage of multiscale modeling for design and manufacturing requires a paradigm shift for the industry. Kassner et al. [308] summarized the future needs of multiscale modeling for metallic and polymeric systems essentially requesting research related to multiscale modeling that deals with discontinuities/defect/microstructures.

Not mentioned in this review but certainly important to multiscale modeling related to solid mechanics are topics such as self-assemblies, thin films, thermal barrier coatings, patterning, phase transformations, nanomaterials design, and semiconductors, which all have an economic motivation for study. Studies related to these types of materials and structures require multiphysics formulations to understand the appropriate thermodynamics, kinetics, and kinematics.

Acknowledgments

The author would like to thank the Center for Advanced Vehicular Systems at Mississippi State University for supporting this work, Jerzy Lesczczynski for his encouragement of documenting the current state of multiscale modeling, and Dean Norman for helping review this article.

References

1. V. E. Panin, Foundations of physical mesomechanics *Phys. Mesomech*., **1** (1998), 5-20.
2. S. Yip, *Handbook of Materials Modeling*, (2005), Springer-Verlag, The Netherlands.
3. E. B. Tadmor et al., Hierarchial modeling in the mechanics of materials, *Int. J. Solids Struct.*, **37** (2000), 379-389.
4. H. Helmholtz, *On the Conservation of Force*, (1847), London.
5. J. C. Maxwell, On the dynamical evidence of molecular constitution of matter, *J. Chem. Soc. London*, **28** (1875), 493-508.
6. L. Onsager, Reciprocal relations in irreversible processes. I, *Phys. Rev*., **37** (1931), 405-426.
7. L. Onsager, Reciprocal relations in irreversible processes. II, *Phys. Rev*, **38** (1931), 2265-2279.

8. C. Eckart, The thermodynamics of irreversible processes. I. The simple fluid, *Phys. Rev*., **58** (1940), 267-269.

9. C. Eckart, The thermodynamics of irreversible processes. IV. The theory of elasticity and anelasticity, *Phys. Rev*., **73** (1948), 373-382.

10. E. Kroner, How the internal state of a physically deformed body is to be described in a continuum theory, *4th Int. Cong. on Rheo.*, (1960).

11. B. D. Coleman and M. E. Gurtin, Thermodynamics with internal state variables, *J. Chem. Phys*. **47** (1967), 597-613.

12. J. R. Rice, Constitutive equations in plasticity, *J. Mech. Phys. Solids*, **9** (1971), 433.

13. J. Kestin, and J. R. Rice, A critical review of thermodynamics, *In. E.B. Stuart (Ed.), Mono Book Corp., Baltimore*, (1970), 275.

14. R. Talreja, Continuum modeling of damage in ceramic matrix composites, *Mech. of Matls*., **12** (1991), 165-180.

15. R. Talreja, Further developments in continuum damage modeling of composites aided by micromechanics, *ASME, App. Mech. Div.*, **150** (1993), 103.

16. R. Talreja, A damage mechanics based approach to durability assessment of composite materials, Composites and Finely Graded Materials, ASME, *Materials Division*, T. Srinivasan et al., Eds., MD Vol-**80** (1997), 151-156.

17. O. A. Hasan and M. C. Boyce, Constitutive model for the nonlinear viscoelastic viscoplastic behavior of glassy polymers**,** *Polymer Eng. and Sci*., **35** 4 Feb (1995), 331-334.

18. H. D. Espinosa et al., A 3-D Finite Deformation Anisotropic Visco-Plasticity Model for Fiber Composites**,** *J. of Composite Matls.*, **35** 5 (2001), 369-410.

19. B. A. Gailly and H. D. Espinosa, Modeling of failure mode transition in ballistic penetration with a continuum model describing microcracking and flow of pulverized media, *Int. J. for Num. Meth. in Eng.*, **54** 3 (2002), 365-398.

20. U. F. Kocks, The relation between polycrystal deformation and single crystal deformation, *Metal. Trans.*, **1** 5 (1970), p. 1121.

21. P. S. Follansbee, Metallurgical applications of shock-wave and high-strain rate phenomena, *L. E. Murr et a., Dekker, NY* (1986), 451-479.

22. P. S. Follansbee and U. F. Kocks, A constitutive description of the deformation of copper based on the use of the mechanical threshold stress as an internal state variable**,** *Acta Materialia*, **36** 1 (1988), 81-93.

23. A. D. Freed, Thermoviscoplastic model with application to copper, *NASA Technical Paper*, *NASA Lewis Research Center*, **2845** (1988), 1-17.

24. D. J. Bammann, An internal variable model of viscoplasticity. *Intl. J. of Eng. Sci.*, **22** 8-10 (1984), 1041-1053.

25. D. J. Bammann, Modeling the Temperature and Strain Rate Dependent Large Deformation of Metals, *Appl. Mech. Rev.*, **43** (1990), S312-319.

26. J.L. Chaboche, Viscoplastic constitutive equations for the description of cyclic and anisotropic behavior of metals, *Bull. de l' Acad., Se'rie Sc. et Techn*., **25** 1 (1977), 33.

27. J. D. Eshelby, The determination of the elastic field of an ellipsoidal inclusion, *Proc. Royal Soc. London, A, Mathl. Phys. Sci.*, **241** 1226 (1957), 376-396.

28. J. D. Eshelby, The elastic field outside an ellipsoidal inclusion, *Proc. Royal Soc. London, A, Mathl. Phys. Sci.*, **252** 1271 (1959), 561-569.

29. R. Hill, Continuum micromechanics of elastoplastic polycrystals, *J. Mech. Phys. Solids*, **13** (1965), 89-101.

30. T. Mura and K. Tanaka, Average stress in matrix and average elastic energy of materials with misfitting inclusions, *Acta Metal.*, **21** (1973), 571-574.

31. T. Mura, *Micromechanics of Defects in Solids*, ISBN 90-247-3343(HB), (1982).

32. B. Budiansky, *Micromechanics: Advances and Trends in Structural and Solid Mechanics*, Pergamon Press, Oxford, (1983), 3-12.

33. S. Nemat-Nasser, and M. Lori, Micromechanics: overall properties of heterogeneous materials, *J. of App. Mech*, **63** 2 (1996), 561.

34. A. M. Gokhale, and S. Yang, Application of image processing for simulation of mechanical response of multi-length scale microstructures of engineering alloys, *Metal. Mat. Trans. A: Phys. Metall. and Mat. Sci.*, **30** 9 (1999), 2369-2381.

35. S. Hao et al., A hierarchical multi-physics model for design of high toughness steels, *J. Computer-Aided Mat. Des.*, **10** (2003), 99-142.

36. Z. P. Bazant and E. P. Chen, Scaling of structural failure, *ASME Applied Mechanics Reviews*, **50** 10 (1997), 593-627.

37. P. W. Bridgman, The compressibility of thirty metals as a function of pressure and temperature, *Proc. of the Amer. Aca. of Arts and Sci*, **58** 5 (1923), 164-242.

38. R. Phillips, *Crystals, Defects and Microstruct.: Model. Across Scales*, (2001) University Cambridge Press.

39. W. K. Liu et al., Introduction to computational nanomechanics and materials, *Nano Mech. and Mat.: Theory, Multiscale Meth. and App.*, (2006) John Wiley and Sons.

40. J. Fish, Bridging the scales in nanoengineering and science, *J. of Nanopart. Rsrch.*, **8** 5 (2006), 577-594

41. J. J. De Pablo, and W. A. Curtin, Multiscale modeling in advanced materials research: Challenges, novel methods, and emerging applications, *MRS Bulletin*, **32** (2007), 905-909.

42. W. Hackbush, *Multi-Grid Methods and Applications*, (1985) Springer-Verlag.

43. S. Kohlhoff, and S. Schmauder, *Atom. Sim. of Matls.: Beyond Pair Potentials*, (1989) Plenum Press, Eds., V. Vitek and D.J. Srolovitz, New York, 411–418.

44. S. Kohlhoff et al., Crack propagation in bcc crystals studied with a combined finite-element and atomistic model, *Phil. Mag. A* **64** (1991), 851–878.

45. E. B. Tadmor et al., Quasicontinuum analysis fo defects in solids, *Phil. Mag. A: Phys. of Cond. Matt., Defects and Mech. Prop.*, **73** 6 (1996), 1529.

46. M. S. Daw, and M. I. Baskes, Embedded-atom method: Derivation and application to impurities, surfaces, and other defects in metals, *Phys. Rev. B*, **29** (1984), 6443-6453.

47. M. S. Daw et al., Embedded atom method--a review of theory and applications, *Matls. Sci. Rep., A Rev. J.*, **9** 7-8 (1993), 251-310.

48. M. Ortiz et al., A finite element method for localized failure analysis, *Comp. Methods Appl. Mech. Eng.* (1987), 189-214.

49. V. B. Shenoy et al., Quasicontinuum Models of Interfacial Structure and Deformation, *Phy. Rev. Lett.*, **80** 4 (1998), 742-745.

50. R. Miller et al., Quasicontinuum simulation of fracture at the atomic scale, *Model. and Sim. in Mat. Sci. and Eng.*, **6** 5 (1998), 607-638.

51. R. Miller et al., Quasicontinuum models of fracture and plasticity, *Eng. Fract. Mech.*, **61** 3-4 (1998), 427-444.

52. V. B. Shenoy et al., An adaptive finite element approach to atomic-scale mechanics—the quasicontinuum method, *J. of the Mech. and Phys. of Solids*, **47** 3 (1999), 611-642.

53. F. F. Abraham et al., Spanning the continuum to quantum length scales in a dynamic simulation of brittle fracture, *Europhysics Letters*, **44** 6 (1998), 783–787.

54. S. J. Plimpton, Lammps code, *J Comp Phys*, **117** (1995), 1-19.

55. R. E. Rudd and J. Q. Broughton, Coarse-grained molecular dynamics and the atomic limit of finite elements, *Phys. Rev. B*, **58** (1998), R5893–R5896.

56. J. Q. Broughton et al., Concurrent coupling of length scales: Methodology and application, *Phys. Review B*, **60** (1999), 2391–2403.

57. E. Lidorikis et al., Coupling Length Scales for Multiscale Atomistics-Continuum Simulations: Atomistically Induced Stress Distributions in Si/Si_3N_4 Nanopixels, *Phys. Rev. Lett.*, **87** 8 (2001), 086104.

58. Z. P. Bazant, Can multiscale-multiphysics methods predict softening damage and structural failure?, *Mechanics, Am. Acad. of Mech.*, **36** 5-6 (2007), 5-12.

59. L. E. Shilkrot et al., Coupled Atomistic and Discrete Dislocation Plasticity, *J. of the Mech. and Physics of Solids*, 50 n 10 (2002) 2085-2106.

60. L. E. Shilkrot et al., Multiscale plasticity modeling: coupled atomistics and discrete dislocation mechanics, *J. of the Mech. and Phy. of Solids*, **52** 4 (2004), 755–787.

61. B. Shiari et al., Coupled Atomistic/Discrete Dislocation Simulations of Nanoindentation at Finite Temperature, *J. of Eng. Mat. and Tech., Trans. of the ASME*, **127** 4 (2005), 358-368.

62. M. P. Dewald, and W. A. Curtin, Multiscale modelling of dislocation/grain boundary interactions. II. Screw dislocations impinging on tilt boundaries in Al, *Phil. Mag.*, **87** 30 (2007), 4615-4641.

63. H. M. Zbib and D. D. L. Rubia, A multiscale model of plasticity, *Int. J. Plast.*, **18** 9 (2002), 1133-1163.

64. M. F. Horstemeyer et al., Design of experiments for constitutive model selection: application to polycrystals elastoviscoplasticity, *Modell. and Sim. in Mat. Sci. and Eng.*, **7** (1999), 253-273.

65. P. R. Dawson, On modeling of mechanical property changes during flat rolling of aluminum, *Int. J. Solids Struct.*, **23** 7 (1987), 947-968.

66. D. Peirce, Asaro, RJ, Needleman, An analysis of nonuniform and localized deformation in ductile single crystals, A *Acta. Metall*., **30** (1982), 1087-1119.

67. M. M. Rashid and S. Nemat-Nasser, Modeling very large plastic flows at very large strain rates for large-scale computation, *Comp. Meth. in App. Mech. and Eng.*, **94** (1990), 201-228.

68. U. F. Kocks et al., *Texture and Anisotropy: Preferred Orientations in Polycrystals and Their Effect on Materials Properties*, Cambridge University Press, (1998).

69. M. S Shephard et al., Automatic construction of 3-D models in multiple scale analysis, *Comp. Mech.*, **17** 3 (1995), 196-207.

70. S. P. Xiao and T. Belytschko, A bridging domain method for coupling continua with molecular dynamics, *Comp. Meth. in Appl. Mech. and Eng*., **193** 17-20 (2004), 1645-1669.

71. G. J. Wagner and W. K. Liu, Coupling of atomistic and continuum simulations using a bridging scale decomposition, *J. of Comp. Phy.*, **190** (2003), 249–274.

72. E. G. Karpov et al., A Green's function approach to deriving non-reflecting boundary conditions in molecular dynamics simulations, *Int. J. for Num. Meth. in Eng.*, **62** 9 (2005), 1250-1262.

73. S. A. Adelman and J. D. Doll, Generalized Langevin equation approach for atom/solid-surface scattering: General formulation for classical scattering off harmonic solids, *J. of Chem. Phys.*, **64** 6 (1976), 2375–2388.

74. W. Cai et al., Minimizing Boundary Reflections in Coupled-Domain Simulations, *Rev. Lett.*, **85** (2000), 3213-3216.

75. W. E. Huang and Z. Y. Huang, A dynamic atomistic-continuum method for the simulation of crystalline materials, *J. of Comp. Phys*., **182** (2002), 234–261.

76. G. J. Wagner et al., *Comp. Meth. in Appl. Mech. and Engng*., **193** 17-20 (2005), 1579-1601.

77. H. S. Park et al., The bridging scale for two-dimensional atomistic/continuum coupling, *Phil. Mag.*, **85** 1 (2005), 79-113.

78. M. F. Horstemeyer et al., A multiscale analysis of fixed-end simple shear using molecular dynamics, crystal plasticity, and a macroscopic internal state variable theory, *Modell. Sim. Mat. Sci. Eng*., **11** (2003), 265-286.

79. J. Fish and W. Chen, Discrete-to-continuum bridging based on multigrid principles, *Comp. Meth. in App. Mech. and Eng.*, **193** 17-20 (2004), 1693-1711.

80. J. Fish, and Z. Yuan, Multiscale enrichment based on partition of unity, *Int. J. of Num. Meth. in Eng.*, **62** 10 (2005), 1341–1359.

81. P. A. Klein and J. A. Zimmerman, Coupled atomistic–continuum simulations using arbitrary overlapping domains, *J. Comp. Phy.*, **213** (2006), 86-116.

82. C. Oskay and J. Fish, Fatigue life prediction using 2-scale temporal asymptotic homogenization *Int. J. for Num. Meth. in Eng.*, **61** 3 (2004), 329-359.

83. J. Fish and C. Oskay, A nonlocal multiscale fatigue model, *Mech. of Adv. Mat. and Struct.*, **12** 6 (2005), 485-500.

84. J. Fish and Q. Yu, Computational mechanics of fatigue and life predictions for composite materials and structures, *Comp. Meth. in App. Mech. and Eng.*, **191** 43 (2002), 4827-4849.

85. E**.** Gal ,et al., A Multiscale Design System for Fatigue Life Prediction, J *Int. J. for Multiscale Comp. Eng.*, **5** 6 (2007), 435-446.

86. G. B. Olson, Systems design of hierarchically structured materials: Advanced steels, *J. of Computer-Aided Mat. Dsgn.*, **4** 3 (1998) 143-156.

87. G. B. Olson, New age of design, *J. of Computer-Aided Mat. Dsgn.*, **7** 3 (2000), 143-144.

88. E. Orowan, Zur kristallplastizität. I, Z. Phys., **89** (1934), 605-659.

89. G. I. Taylor, The Mechanism of Plastic Deformation of Crystals. Part I. Theoretical, *Proc. R. Soc. London Ser.* **A145 855** (1934), 362-387.

90. M. Z. Polyani, Űber eine Art Gilterstorung die einen Kristall plastisch machen konnte, *Z. Phys.*, **89** (1934), 660-664.

91. F. Nabarro, Mathematical theory of stationary dislocations, *Adv. in Phy.*, **1** (1952), 269.

92. J. M. Burgers, Some considerations on the fields of stress connected with dislocations in a regular crystal lattice. I*Proc. Kon. Ned. Akad. Wetenschap.*, **42** (1939), 293.

93. E. O. Hall, The Deformation and Ageing of Mild Steel: III Discussion of Results, *Proc. Phys. Soc.*, **B64** (1951), 747-753.

94. N. J. Petch, The cleavage strength of polycrystals, *J. Iron Steel Ins.*, **174** (1953), 25.

95. M. Ashby, *Strength. Meth. in Crystals,* Eds. A. Kelly and R.B. Nicholson, (1971) 137.

96. F. C. Frank, The influence of dislocations on crystal growth, *Disc. Faraday Soc.*, **5** (1949), 48.

97. F. C. Frank, Crystal dislocations. elementary concepts and definitions, *Phil. Mag.*, **42** (1951), 809.

98. W. T. Read, *Dislocations in Crystals*, McGraw-Hill, New York, NY, (1953).

99. D. A. Hughes et al., Near surface microstructures developing under large sliding loads, *J. Matls. Eng. Perf.*, **3** (1994), 459-475.

100. D. A. Hughes and W. D. Nix, The absence of steady-state flow during large strain plastic deformation of some Fcc metals at low and intermediate temperatures, *Metall and Matl. Trans. A*, **19** (1988), 3013-3024.

101. N. A. Fleck et al., Strain gradient plasticity: theory and experiment, *Acta Materialia*,, **42** 2 (1994), 475-487.

102. J. S. Stolken and A. G. Evans, A microbend test method for measuring the plasticity length scale, *Acta Materialia*, **46** 14 (1998), 5109.

103. W. D. Nix, Mechanical properties of thin films, *Metall. Trans.* **20A** (1989), 2217-2245.

104. M. S. De Guzman et al., The role of indentation depth on the measured hardness of materials, *Matls. Rsrch. Sym. Pro.*, **308** (1993), 613-618.

105. N. A. Stelmashenko etal., Microindentations on W and Mo oriented single crystals: an STM study, *Acta. Metall. Mater.*, **41** (1993), 2855-5865.

106. Q. Ma and D. R. Clarke, Size dependent hardness of silver single crystals, *J. Mater. Research*, **10** (1995), 853-863.

107. W. J. Poole et al., Micro-Hardness of annealed and work-hardened copper polycrystals, *Scripta Metall. Mater*., **34** (1996), 559-564.

108. K. W. McElhaney et al., Determination of indenter tip geometry and indentation contact area for depth-sensing indentation experiments, *J. Mater. Res.*, **13** (1998), 1300-1306.

109. D. J. Lloyd, Particle reinforced aluminium and magnesium matrix composites, *Int. Mater. Rev.*, **39** (1994), 1-23.

110. G. Elssner et al., The influence of interface impurities on fracture energy of UHV diffusion bonded metal-ceramic bicrystals, *Scripta Metall. Mater*., **31** (1994), 1037-1042.

111. A. Griffith,. A. *Philosophical Transactions, Roy. Soc. of London* A **221** (1921). 163-198.

112. W. C. Roberts-Austen, On Certain Mechanical Properties of Metals Considered in relation to the Periodic Law, *Phil. Trans. R. Soc. London A*, **179** (1888), 339-349.

113. F. A. McClintock, A criterion for ductile fracture by the growth of holes, *J. of App. Mech.* **35** (1968), 363-371.

114. A. Gangalee and J. Gurland, On the fracture of silicon particles in aluminum–silicon alloys, *Trans. Metall. Soc. of AIME*, **239** (1967), 269-272.

115. M. F. Horstemeyer and S. Ramaswamy, On Factors Affecting Localization and Void Growth in Ductile Metals: A Parametric Study, *Int. J. Damage Mech.*, **9** (2000), 6-28.

116. M. F. Horstemeyer et al., Micromechanical finite element calculations of temperature and void configuration effects on void growth and coalescence, *Int J. Plasticity*, **16** (2000).

117. G. P. Potirniche et al., A molecular dynamics study of void growth and coalescence in single crystal nickel, *Int. J. of Plasticity*, **22** 2 (2006), 257-278.

118. G. P. Potirniche et al., Lattice orientation effects on void growth and coalescence in fcc single crystals, *Int. J. of Plasticity*, **22** 5 (2006), 921-942.

119. G. P. Potirniche and M. F. Horstemeyer, Lattice orientation effects on void growth and coalescence in fcc single crystals, *Phil. Mag. Lett.*, **86** 3 (2006), 185-193.

120. G. P. Potirniche et al., Atomistic modelling of fatigue crack growth and dislocation structuring in FCC crystals, *Proce. of the Roy.Soc. A, London*, **462** (2006), 3707-3731.

121. M. K. Jones et al., A multiscale analysis of void coalescence in nickel *J. Eng. Matls. Tech.*, **129** (2007), 94-104.

122. H. Neuber *Theory of notch stresses*. (1958) Berlin: Springer.

123. R. E. Peterson. *Metal Fatigue*, Eds. G. Sines and J. L. Waisman, McGraw-Hill, New York, NY, (1959), 293–306.

124. G. Harkegard, Application of the finite element method to cyclic loading of elastic-plastic structures containing effects *Int. J. Frac*., **9** (1973), 322.

125. R. A. Smith and K. J. Miller, Fatigue cracks at notches, *Int. J. of Mech. Sci.*, **19** 1 (1977), 11-22.

126. R. A. Smith et al., Experimental and theoretical fatigue-crack propagation lives of variously notched plates, *J. of Strain Ana. for Eng. Dsgn.*, **9** 2 (1974), 61-66.

127. J. Lankford and F. N. Kusenberger, Initiation of fatigue cracks in 4340 steel, *Met. Trans*., **4** (1973), 553-559.

128. J. Lankford, Inclusion-Matrix debonding and fatigue crack intiation in low alloy steel, *Met. Trans*., **4** (1976), 155-157.

129. J. Lankford et al., The influence of crack tip plasticity in the growth of small fatigue cracks, *Metall. Trans. A*, **4** (1984), 1459-1588.

130. M. J. Couper et al., Casting defects and the fatigue behaviour of an aluminium casting alloy, *Fat. Frac. Eng. Mat. Struc*., **13** (1990), 213-227.

131. J. F. Major, Porosity control and the fatigue behavior in A356-T61 aluminum alloy, *AFS Trans*., **102** (1994), 901-906.

132. D. L. Davidson et al., The effects on fracture toughness of ductile-phase composition and morphology in Nb-Cr-Ti and Nb-Siin situ composites, *Metall. and Matls. Trans. A: Physl. Metall. and Matls. Sci.*, **27** 9 (1996), 2540-2556.

133. P. J. Laz and B. M. Hillberry, Fatigue life prediction from inclusion initiated cracks, *Int. J. of Fatigue*, **20** 4 (1998), 263-270

134. K. A. Gall et al., The debonding and fracture of Si particles during the fatigue of a cast Al-Si alloy, *Met. Trans A.*, **30** (1999), 3079-3088.

135. K. A. Gall et al., High cycle fatigue mechanisms in a cast AM60B magnesium alloy , *Fatigue Frac. Eng. Mat. Struct.*, **23** (2000), 159-172.

136. K. A. Gall et al., Finite element analysis of the stress distributions near damaged Si particle clusters in cast Al–Si alloys, *Mech. Mater*., **32** 5 (2000), 277-301.

137. X. S. Wang et al., Low-cycle fatigue small crack initiation and propagation behaviour of cast magnesium alloys based on in-situ SEM observations, *Phil. Mag.*, **86** 11 (2006), 1581-1596.

138. S. Kumar and W. A. Curtin, Crack interaction with microstructure, *Materials Today*, **10** 9 (2007), 34.

139. M. M. Shenoy et al., Modeling effects of nonmetallic inclusions on LCF in DS nickel-base superalloys, *Int. J. Fatigue*, **27** (2005), 113-127.

140. M. M. Shenoy et al., Estimating fatigue sensitivity to polycrystalline Ni-base superalloy microstructures using a computational approach, *Fat. Fract. Eng. Mat. Struct.*, **30** 10 (2007), 889-904.

141. D. L. McDowell, Simulation-assisted materials design for the concurrent design of materials and products, *The J. of Mins., Metls. & Matls. Soc.*, **59**. 9 (2007), 21-25.

142. J. Fan et al., Cyclic plasticity across micro/meso/macroscopic scales, *Proc. R. Soc. London A*, **460** (2004), 1477-1503.

143. M. F. Horstemeyer, Damage influence on Bauschinger effect of a cast A 356 aluminum alloy, *Scripta Materialia*, **39** 11 (1998), 1491-1495.

144. M. F. Horstemeyer and M. I. Baskes, Atomistic Finite Deformation Simulations: A Discussion on Length Scale Effects in Relation to Mechanical Stresses, *J. Eng. Matls. Techn. Trans. ASME*, **121** 2 (1999), 114-119.

145. M. F. Horstemeyer et al., Length scale and time scale effects on the plastic flow of fcc metals, *Acta Mateialia*., **49** (2001), 4363-4374.

146. M. F. Horstemeyer, Mapping failure by microstructure-property modeling, *Journal of Metals*, (2001b) ed. J.J. Hoyt.

147. M. F. Horstemeyer et al., *From Atoms to Autos: Part 2 Fatigue Modeling*, Sandia National Laboratories Report, SAND2001-8661, (2001).

148. M. F. Horstemeyer et al., J *Prospects in Mesomechanics*, Ed. G. Sih, *Theoretical and Applied Fracture Mechanics*, **37** 1-3 (2001), 49-98.

149. M. F. Horstemeyer et al., A large deformation atomistic study examining crystal orientation effects on the stress–strain relationship *Int. J. Plasticity*, **18** (2002), 203-209.

150. M. F. Horstemeyer et al., Torsion/simple shear of single crystal copper, *J. of Eng. Matls. and Tech.*, **124** (2002), 322-328.

151. M. F. Horstemeyer, *Physically Motivated Modeling of Deformation-Induced Anisotropy*, PhD thesis, Georgia Institute of Technology, (1995).

152. W. W. Gerberich et al., Interpretations of indentation size effects, J. *Applied Mechanics*, **69** 4 (2002), 443-452.

153. J. Fan et al., Cyclic plasticity at pores and inclusions in cast Al–Si alloys, *Eng. Fract. Mech.*, **68** 15 (2001), 1687-1706.

154. J. Fan et al., Cyclic plasticity at pores and inclusions in cast Al–Si alloys, *Eng. Fract. Mech.*, **70** 10 (2003), 1281-1302.

155. S. Johnston et al., Three-dimensional finite element simulations of microstructurally small fatigue crack growth in 7075 aluminium alloy, *Fatigue Fract. Eng. Matl. Struct.*, **29** (2006), 597-605.

156. K. A. Gall et al., On the driving force for fatigue crack formation from inclusions and voids in a cast A356 aluminum alloy, *Int.J. of Fracture*, **198** 3 (2001), 207-233.

157. V. S. Deshpande et al., Discrete dislocation plasticity modeling of short cracks in single crystals, *Acta Materialia*, **51** 1 (2003), 1-15.

158. V. S. Deshpande et al., Scaling of discrete dislocation predictions for near-threshold fatigue crack growth, *Acta Materialia*, **51** 15 (2003b), 4637-4651.

159. T. Morita and H. Tsuji, Zairyo, *J. of the Soc. of Matls. Sci., Japan*, **53** 6 (2004), 647-653.

160. I. N. Mastorakos and H. M. Zbib, MD simulations of dislocation-crack interaction during fatigue, *J. of ASTM Int.*, **4** 8 (2007) Page Number??????????.

161. S. Groh et al., Fatigue crack growth from a cracked elastic particle into a ductile matrix, *Phil. Mag*., (2008) accepted.

162. D. L. McDowell and G. B. Olson, Concurrent design of hierarchical materials and structures, submitted to *Sci. Model. and Sim. (*2008).

163. A. Ramasubramaniam and E. A. Carter, Coupled quantum—atomistic and quantum—continuum mechanics methods in materials research, *MRS Bulletin*, **32** (2007), 913-918.

164. G. Lu and E. Kaxiras, *Handbook of Theoretical and Computational Nanotechnology*, Eds. Rieth et al., 22, Am. Sci. Publ., Stevenson Ranch, Ca, (2004).

165. N. Choly et al., Multiscale simulations in simple metals: A density-functional-based methodology, *Phys. Rev. B*., **71** (2005), 094101

166. G. Lu et al., From electrons to finite elements: a concurrent multiscale approach for metals, *Physl. Rev. B, Cond. Matt. and Matls. Phys.*, **73** (2006), 024108.

167. F. Ercolessi and J. Adams, Interatomic potentials from first-principles calculations: the force-matching method, *Europhysics Letters*, **26** (1994), 583–588.

168. Y. Li et al., Embedded-atom-method tantalum potential developed by the force-matching method , *Phyl. Rev. B, Cond. Matt.r and Matls. Phys.*, **67** (2003), 125101.

169. N. Govind et al., Accurate ab initio energetics of extended systems via explicit correlation embedded in a density functional environment, *Chem. Phys. Lett*, **295** (1998), 129.

170. Y. A. Wang et al., Orbital-free kinetic-energy functionals for the nearly free electron gas, *Phys. Rev. B*, **58** (1998), 13465.

171. Y. A. Wang et al., Orbital-free kinetic-energy density functionals with a density-dependent kernel, *Phys. Rev. B*, **60** (1999), 16350.

172. T. Kluner et al., Prediction of electronic excited states of adsorbates on metal surfaces from first principles, *Phys. Rev. Lett,*, **86** 26 (2001), 5954.

173. G. Cs´anyi et al., "Learn on the Fly": A hybrid classical and quantum-mechanical molecular dynamics simulation, *Physl. Rev. Lett.*, **93** (2004), 175503.

174. M. I. Baskes, Application of the embedded-atom method to covalent materials: a semiempirical potential for silicon, *Physl. Rev. Lett.*, **59** 23 (1987), 2666–2669.

175. M. I. Baskes et al., Semiempirical modified embedded-atom potentials for silicon and germanium, *Physl. Rev. B*, **40** 9 (1989), 6085–6100.

176. M. I. Baskes et al., Atomistic calculations of composite interfaces, *Modell. Simul. Mater. Sci. Eng.*, **2** (1994), 505–518.

177. M. I. Baskes and R. A. Johnson, Modified embedded atom potentials for HCP metals, *Modell. Simul.Mater. Sci. Eng.*, **2** 1 (1994), 147–163.

178. B. Jelinek et al., Modified embedded-atom method interatomic potentials for the Mg-Al alloy system, *Physl. Rev. B*, **75** 5 (2007), 054106.

179. M. S. Daw and M. I. Baskes, Semiempirical, Quantum Mechanical Calculation of Hydrogen Embrittlement in Metals, *Physl. Rev. Lett.*, **50** (1983), 1285–1288.

180. M. Q. Chandler, , Horstemeyer, MF, Baskes, MI, Gullett, PM, Wagner, GJ, Jelinek, B, Hydrogen effects on nanovoid nucleation in face-centered cubic single -crystals, Acta Materialia, **56** 1 (2008), 95-104.

181. M. Q. Chandler et al.,, Hydrogen effects on nanovoid nucleation at nickel grain boundaries, *Acta Materialia*, **56** 3 (2008), 619-631.

182. H. Fang et al., Atomistic simulations of Bauschinger effects of metals with high angle and low angle grain boundaries, *Comp. Meth. in App. Mech. and Eng.*, **193** (2004), 1789-1802.

183. K. Solanki et al., Multiscale study of dynamic void collapse in single crystals, *Mech. of Matls.*, **37** (2005), 317-330.

184. D. Farkas, Atomistic Studies of Intrinsic Crack-Tip Plasticity, *MRS Bulletin*, **25** 5 (2000), 35-38.

185. D. Farkas, Atomistic Mechanisms of Fatigue in Nanocrystalline Metals, *Phys. Rev. Letters*, **94** 16 (2005), 165502.

186. A. Luque et al., Molecular dynamics simulation of crack tip blunting in opposing directions along a symmetrical tilt grain boundary of copper bicrystal, *Fatigue and Fracture of Eng. Matls. and Struct.*, **30** 11 (2007), 1008-1015.

187. A. Brandt, *Multiscale and Multiresolution Methods: Theory and Applications*, Springer-Verlag, Heidelberg, (2001).

188. E. Weinan and B. Engquist, Heterogeneous multiscale methods, *Comm. Math. Sci.*, **1** 1 (2003), 87-132.

189. G. I. Barenblatt, *Scaling*, Cambridge Texts in Applied Mathematics, (2003).

190. A. Carpinteri et al., Cohesive crack model description of ductile to brittle size-scale transition: dimensional analysis vs. renormalization group theory, *Eng. Fracture Mech.*, **70** 14 (2003), 1809-1839.

191. Y. T. Cheng and C. M. Cheng, Fundamentals of nanoindentation and nanotribology, *Matls. Rsrch. Soc. Sym. – Proce.*, **522** (1998), 139-144.

192. N. Ansini et al., Multi-scale analysis by Gamma-convergence of a one-dimensional non-local functional related to a shell-membrane transition, *SIAM Journal on Mathematical Analysis*, **38** 3 (2006), 944-976.

193. B. B. Mandelbrot et al., Fractal character of fracture surfaces of metals, *Nature*, **308** (1984), 721 – 722.

194. B. B. Mandelbrot, *The Fractal Geometry of Nature*, W. H. Freeman and Company, (1982).

195. D. M. Mark and P. B. Aronson, *Mathematical Geology*, Springer, (1984).

196. T. Chelidze and Y. Guguen, Evidence of fractal fracture, *Int. J. of Rock Mech. and Mining Sci.*, **27** 33 (1990), 223-225.

197. A. B. Mosolov et al., Fractal Fracture of Brittle Bodies during Compression, *Soviet Phys.*, Doklady, Plenum Publishing, **37** 55 (1992), 263-265.

198. A. V. Dyskin, *Int. Journal of Solids and Structures, Micromechanics of Materials*, **42** 2 (2005), 477-502.

199. S. Graham and N. Yang, Representative volumes of materials based on microstructural statistics, *Scripta Materialia*, **48** 3 (2003), 269-274.

200. S. Lee and R. Rao, Scale-based formulations of statistical self-similarity in images, *Proc. Int. Conf. on Image Processing*, ICIP, **4** (2004), 2323-2326.

201. J. Fish and A. wagiman, adaptive, multilevel, and hierarchical computational strategies, *Winter Annual Meeting of the American Society of Mechanical Engineers*, **157** (1992), 95-117.

202. J. Fish and Yuan, Multiscale enrichment based on partition of unity for nonperiodic fields and nonlinear problem, *Comp. Mech.*, **40** 2 (2007), 249-259.

203. M. A. Nuggehally et al., Adaptive Model Selection Procedure for Concurrent Multiscale Problems, Int. J. for Multiscale Comp. Eng., **5** 5 (2007), 369-386.

204. G. W. He et al., Multiscale coupling: challenges and opportunities, *Prog. in Nat. Sci.*, **14** (2004), 463-466.

205. H. Y. Wang et al., Multiscale coupling in complex mechanical systems, *Chem. Eng. Sci*, **59** (2004), 1677-1686.

206. J. W. Essam, Phase transitions and critical phenomena, *Conf. Proc. Cambridge Phil Soc*., (1970), 523-533.

207. S. Greenspoon, Finite-size effects in one-dimensional percolation: a verification of scaling theory, *Canadian J. of Phys.*, **57** 4 (1979), 550-552.

208. H. Kestin, *Percolation Theory for Mathematicians*, Bull. Amer. Math. Soc., **11** (1984), 404-409.

209. Y. Otsubo, Elastic percolation in suspensions flocculated by polymer bridging, *Langmuir*, **6** 1 (1992), 114-118.

210. D. F. Leclerc and J. A. Olson, A percolation-theory model of lignin degradation, *Macromolecules*, **25** 6 (1992), 1667-1675.

211. R. Fu et al., Interpretation of porosity effect on strength of highly porous ceramics, *Scripta Metall. et Matl.*, **25** 7 (1991), 1583-1585.

212. M. Ostoja-Starzewski, Mechanics of damage in a random granular microstructure: Percolation of inelastic phases, *Int. J. of Eng. Sci*., **27** 3 (1989), 315-326.

213. Y. L. Bai et al., Statistical mesomechanics of solid, linking coupled multiple space and time scales, *App. Mech. Rev*., **58** (2005), 372-388.

214. L. E. Reichl, *A Modern Course in Statistical Physics*, University of Texas Press, Austin, (1980).

215. B. Zhang et al., Microstructural effects on high-cycle fatigue-crack initiation in A356.2 casting alloy, *Metall. and Matls. Trans. A*, **30** **10** (1999), 2659-2666.

216. M. F. Horstemeyer and P. Wang, Cradle-to-grave simulation-based design incorporating multiscale microstructure-property modeling: Reinvigorating design with science, *J. Computer-Aided Matls. Dsgn.*, **10** (2003), 13-34.

217. R. A. Fisher, *Statistical Methods for Research Workers*, (1935) Oliver and Boyd, Edinburg.

218. R. A. Fisher, *The Design of Experiments*, (1935) Oliver and Boyd, Edinburg.

219. G. Taguchi, *System of Experimental Design: I and II*, UNIPUB, New York, (1987).

220. G. Taguchi, *Reports of Statistical Application Research*, JUSE, **6** (1960), 1-52.

221. M. F. Horstemeyer and AM Gokhale, A void-crack nucleation model for ductile metals, *Int. J. of Solids and Struct.*, **36** (1999), 5029-5055.

222. M. F. Horstemeyer et al., Using a micromechanical finite element parametric study to motivate a phenomenological macroscale model for void/crack nucleation in aluminum with a hard second phase, *Mech. of Matls.*, **35** (2003), 675-687.

223. J. C. Mauro and A. K. Varshneya, Multiscale modeling of $GeSe_2$ glass structure, *J. Amer. Ceramic Soc*., **89** 7 (2006), 2323-2326.

224. J. C. Mauro and A. K. Varshneya, Ab initio modeling of volume–temperature curves for glassforming systems, *J. Non-Crystalline Solids*, **353** 13-15 (2007), 1226-1231.

225. R. Krishnamurthy et al., Oxygen diffusion in yttria-stabilized zirconia: a new simulation model, *J. Amer. Ceramic Soc*., **87** 10 (2004), 1821-1830.

226. A. Hansen et al., Roughness of crack interfaces, *Phys. Rev. Lett*, **66** 19 (1991), 2476-2479.

227. J. Schmittbuhl et al., Roughness of interfacial crack fronts: stress-weighted percolation in the damage zone, *Phys. Rev. Lett.*, **90** 4 (2003), 045505.

228. A. Hansen and J. Schmittbuhl, Origin of the universal roughness exponent of brittle fracture surfaces: stress-weighted percolation in the damage zone *Phys. Rev. Lett.*, **90** 4 (2003), 045504.

229. L. Chong, and L. B. Ray, Whole-istic Biology, *Science*, **295** 5560 (2002), 1661.

230. D. N. Theodorou, Hierarchical modeling of amorphous polymers, *Comp. Phys. Comm.*, **169** 1-3 (2005), 82-88.

231. A. E. Ismail et al., Using wavelet transforms for multiresolution materials modeling, *Comp. and Chem. Eng., Cont. of Multiscale and Distributed Proc. Sys.*, **29** 4, (2005), 689-700.

232. J. Bicerano et al., Polymer modeling at the dow chemical company, *J. of Macromolecular Sci. – Poly. Rev.*, **44** 1 (2004), 53-85.

233. Q. Yu and J. Fish, Multiscale asymptotic homogenization for multiphysics problems with multiple spatial and temporal scales: a coupled thermo-viscoelastic example problem, *Int. J. of Solids and Struct.*, **39** 26 (2002), 6429-6452.

234. S. Curgul et al., Molecular Dynamics Simulation of Size-Dependent Structural and Thermal Properties of Polymer Nanofiber, *Macromolecules*, **40** 23 (2007), 8483-8489.

235. J. C. Halpin et al., Time Dependent Static Strength and Reliability for Composites, *Compo. Mater*, **4** (1970), 462-474.

236. J. C. Halpin, Structure-Property Relations and Reliability Concepts, *J. of Compo. Matls.*, **6** (1972), 208-231.

237. H. T. Hahn and S. W. Tsai, On the Behavior of Composite Laminates After Initial Failures, *J. of Comp. Matls.*, **8** 3 (1974), 288-305.

238. J. C. Halpin and J. L. Kardos, The Halpin-Tsai equations: a review, *Poly. Eng. and Sci.*, **16** 5 (1976), 344-352.

239. H. T. Chang, and D. H. Allen, Predicted dynamic response of a composite beam with history-dependent damage, *Comp. and Struct.*, **26** 4 (1987), 575-580.

240. D. H. Allen et al., A cumulative damage model for continuous fiber composite laminates with matrix cracking and interply delaminations, *ASTM Sp. Tech. Pub.*, **972** (1988), 57-80.

241. F. Costanzo and D. H. Allen, Micromechanics and homogenization of inelastic composite materials with growing cracks, J. *of the Mech. and Phys. of Solids*, **44** 3 (1996), 333-370.

242. D. Krajcinovic, Constitutive equations for damaging materials, *J. App. Mech.*, (1983)

243. D. Krajcinovic, Continuum damage mechanics: when and how?, *Int. J. Damage Mech.*, **4** 3 (1995), 217.

244. D. Krajcinovic, *Damage Mechanics*, Noth-Holland, New York, NY, (1996).

245. J. Fish and K. Shek, Multiscale analysis of composite materials and structures, *Compo. Sci. and Tech.*, **60** 12-13 (2000), 2547-2556.

246. J. Fish and Q. Yu, Multiscale damage modeling for composite materials: Theory and computational framework, *Int. J. for Num. Meth. in Eng., 5th US Nat. Cong. on Comp. Mech.*, **52** 1-2 (2001), 161-191.

247. V. Belsky et al., Computer-aided multiscale modeling tools for composite materials and structures *Comp. Syst. in Eng.: An Int. J.*, **6** 3 (1995), 213-223.

248. B. Hassani and E. Hinton, A review of homogenization and topology opimization II—analytical and numerical solution of homogenization equations, *Comp. and Struct*, **69** 6 (1998), 719-738.

249. B. Hassani and E. Hinton, *Comp. and Struct.*, **69** 6 (1998), 707-717.

250. B. Hassani and E. Hinton, A review of homogenization and topology optimization III—topology optimization using optimality criteria, *Comp. and Struct.*, **69** 6 (1998), 739-756.

251. P. B. Lourenco et al., Analysis of masonry structures: review of and recent trends in homogenization techniques, *Canadian J. of Civil Eng., Special Issue on Masonry*, **34** 11 (2007), 1443-1457.

252. K. Matous et al., Multiscale cohesive failure modeling of heterogeneous adhesives, *J. of the Mech. and Phys. of Solids*, **56** 4 (2008), 1511.

253. J. Aboudi, Micromechanical analysis of composites by the method of cells, *App. Mech. Rev.*, **47** 7 (1989), 193-221.

254. J. Aboudi, The generalized method of cells and high-fidelity generalized method of cells micromechanical models? a review, J *Mech. of Adv. Matls. and Struct.*, **11** 4-5 (2004), 329-366.

255. M. Paley, and J. Aboudi, Micromechanical analysis of composites by the generalized cells model, *Mech. of Matls.*, **14** 2 (1992), 127–139.

256. T. O. Williams and T. B. Tippetts, Materials Damage Prognosis, *Pro. of a Sym. of the Matls. Sci. and Tech. 2004 Conf.*, (2004), 95-101.

257. D. Qian et al., Mechanics of carbon nanotubes, *App. Mech. Rev.*, **55** 6 (2002), 495-532.

258. A. Maiti, Multiscale modeling with carbon nanotubes, *Microelectronics Journal*, **39** 2 (2008), 208-221.

259. G. Friesecke, and R. D. James, A scheme for the passage from atomic to continuum theory for thin films, nanotubes and nanorods, *J. Mech. Phys. Solids*, **48** (2000), 1519-1540.

260. J. Wescott et al., Atomistic, mesoscale and finite element simulation of nanofube dispersion in polymers, *VDI Berichte*, **1940** (2006), 23-24.

261. K. Laganà, et al., Multiscale modeling of the cardiovascular system: application to the study of pulmonary and coronary perfusions in the univentricular circulation, *J. Biomech.*, **38** 5 (2004), 1129-141.

262. H. B. Tho et al., Multi-scale characterization and modeling of human cortical bone, *Mat. Rsrch. Soc. Sym. Pro.*, (2006), 898.

263. E. Budyn, and T. Hoc, Multi-scale modeling of human cortical bone: aging and failure studies, *Mat. Rsrch. Soc. Sym. Pro.- Mech. of Bio. and Bio-Inspired Matls.*, **975** (2006), 27-32.

264. A. Fritsch, and C. Hellmich, Universal microstructural patterns in bone: micromechanics-based prediction of anisotropic material behavior, *Matls. Rsrch. Soc. Sym. Pro.-Mech. of Bio. and Bio-Inspired Matls.*, **975** (2006), 128-134.

265. D. Porter, Pragmatic multiscale modeling of bone as a natural hybrid nanocomposite, *Matls. Sci. and Eng. A*, **365** 1-2 (2004), 38-45.

266. J. L. Katz et al., Multiscale mechanics of hierarchical structure/property relationships in calcified tissues and tissue/material interfaces, *Matls. Sci. and Eng. C-Next Gen. Biomatls.*, **27** 3 (2007), 450-468.

267. Z. A. Taylor, and K. Miller, Constitutive modeling of cartilaginous tissues: A review, *J. of App. Biomech.*, **22** 3 (2006), 212-229.

268. C. Hellmich et al., Can the diverse elastic properties of trabecular and cortical bone be attributed to only a few tissue-independent phase properties and their interactions?, *Biomech. and Model. in Mechanobio.*, **2** 4 (2004), 219-238.

269. D. Taylor, Fracture and repair of bone: a multiscale problem, *J. of Matls. Sci.*, **42** 21 (2007), 8911-8918.

270. M. Kawagai et al., Multi-scale stress analysis of trabecular bone considering trabeculae morphology and biological apatite crystallite orientation, *J. of the Soc. of Matls. Sci.*, Japan, **55** 9 (2006), 874-880.

271. C. Imielinska et al., Multi-scale modeling of trauma injury, *Lect. Notes in Comp. Sc.,,LNCS - IV, Computational Science - ICCS 2006*, **3994** (2006), 822-830.

272. J. B. Bassingthwaighte et al., Strategies and tactics in multiscale modeling of cell-to-organ systems, *Pro. of the IEEE*, **94** 4 (2006), 819-830.

273. E. C. N. Silva et al., Modeling bamboo as a functionally graded material: lessons for the analysis of affordable materials, *J. of Matls. Sci.*, **41** 21 (2006) 6991-7004.

274. A. Makela, Process-based modeling of tree and stand growth: towards a hierarchical treatment of multiscale processes, *Canadian J. of Forest Rsrch.*, **33** 3 (2003), 398-409.

275. J. H. Panchal et al., A strategy for simulation-based design of multiscale, multi-functional products and associated design processes, *Pro. of the ASME Int. Design Eng. Tech. Con. and Comp. and Info. in Eng. Con. - DETC2005*, **2B**, (2005), 845-857.

276. G. B. Olson, Computational design of hierarchically structured materials, *Science*, **277** 5330 (1997), 1237-1242.

277. H. J. Jou et al., Computer simulations for the prediction of microstructure/property variation in aeroturbine disks, *Superalloys 2004*, Eds. Green et al., (2004), 877-886.

278. G. B. Olson, Advances in theory: Martensite by design, *Matls. Sci. and Eng. A*, **25** (2006), 48-54.

279. F. Mistree et al., Robust concept exploration methods in materials design, *9th AIAA/ISSMO Sym. on Multidisci. Ana. and Opt.*, AIAA, (2002), 5568.

280. C. C. Seepersad et al., Design of Multifunctional Honeycomb Materials, *9th AIAA/ISSMO Sym. on Multidisci. Ana. and Opt.*, AAIA, (2002), 5626.

281. C. C. Seepersad et al., Robust design of cellular materials with topological and dimensional imperfections, *J. of Mech. Design*, **128** 6 (2006), 1285-1297.

282. R. Von Mises, Mechanik der festen korper im plastisch deformablen zustand, *Göttin. Nachr. Math. Phys.*, **1** (1913), 582-592.

283. D. J. Bammann and E. C. Aifantis, A model for finite-deformation plasticity, *Acta Mechanica*, **69** (1987), 97-117.

284. D. J. Bammann and E. C. Aifantis, A damage model for ductile metals *Nuc. Eng. and Design*, **116** (1989), 355-362.

285. D. J. Bammann et al., Failure in ductile materialsusing finite element methods, *Structl. Crashworthiness and Failure,* Eds. T. Wierzbicki et al., Elsevier Applied Science, The Universities Press (Belfast) Ltd., (1993).

286. M. F. Horstemeyer et al., Numerical, experimental, nondestructive, and image analyses of damage progression in cast A356 aluminum notch tensile bars, *Theotl. and App. Fracture Mech.*, **39** 1 (2003), 23-45.

287. K. Solanki et al., Integration of microstructure-property relationships in an internal state variable plasticity and damage constitutive model for reliability-based optimization in engineering design. (2008) *submitted to Journal of Design Engineering.*

288. E. Acar et al., Uncertainty Analysis of Damage Evolution Computed through Microstructure-Property Relations, *ASME 34th Design Automation Conference (DAC), New York, NY*, (2008).

289. X. Yin, , Lee, S, Chen, W, Liu, WK, Horstemeyer, MF *A Multiscale Design Approach with Random Field Representation of Material Uncertainty*, ASME DETC08, New York, NY, (2008).

290. M. D. Dighe et al., Effect of loading condition and stress state on damage evolution of silicon particles in an Al-Si-Mg-Base cast alloy, *Metall. and Matls. Trans. A*, **33** (2002), 555-565.

291. M. D. Dighe et al., Effect of temperature on silicon particle damage in A356 alloy, *Metall. and Matls. Trans. A*, **29** (1997), 905-908.

292. M. D. Dighe et al., Effect of strain rate on damage evolution in a cast Al-Si-Mg base alloy, *Metall. and Matls. Trans. A*, **31** (2000), 1725-1731.

293. M.F. Horstemeyer et al., Modeling stress state dependent damage evolution in a cast Al-Si-Mg aluminum alloy, *Theotl. and App. Fracture Mech.*, **33** (2000), 31-47.

294. J. B. Jordon et al., Damage and stress state influence on the Bauschinger effect in aluminum alloys, *Mech. of Matls.*, **39** (2007), 920-931.

295. H. E. Kadiri et al., Fatigue crack growth mechanisms in high-pressure die-cast magnesium alloy, *Metall. and Mat. Trans.,A,* **39** 1 (2008), 190-205.

296. H. E. Kadiri et al., Identification and modeling of fatigue crack growth mechanisms in a die-cast AM50 magnesium alloy, *Acta Materialia*, **54** 19 (2006), 5061-5076.

297. M. F. Horstemeyer et al., High cycle fatigue of a die cast AZ91E-T4 magnesium alloy, *Acta Materialia*, **52** (2004), 1327-1336.

298. D. L. McDowell et al., Microstructure-based fatigue modeling of cast A356-T6 alloy, *Eng. Fracture Mech.*, **70** (2003), 49-80.

299. Y. Xue et al., Micromechanisms of multistage fatigue crack growth in a high-strength aluminum alloy, *Acta Materialia*, **55** 6 (2007), 1975-1984.

300. Y. Xue et al., Multistage fatigue modeling of cast A356-T6 and A380-F aluminum alloys, *Metall. and Matls. Trans.*, **38B** (2007), 601-606.

301. Y. Xue et al., Microstructure-based multistage fatigue modeling of aluminum alloy 7075-T651, *Eng. Fract. Mech.*, **74** (2007), 2810-2823.

302. Y. Xue et al., Microstructure-based multistage fatigue modeling of a cast AE44 magnesium alloy, *Int. J. of Fatigue*, **29** (2007), 666-676.

303. P. C. Paris and F. Erdogan, A critical analysis of crack propagation laws, *Trans. ASME, J. Basic Eng*., **D85** (1963), 528-534

304. J. C. Newman, FASTRAN-2: A fatigue crack growth structural analysis program, *NASA-TM-104159*, (1992), NASA Langley Research Center.

305. J. C. Newman, A review of modeling small-crack behavior and fatigue-life predictions for aluminum alloys, *J. Fatigue and Fract. of Eng. Mat. and Struct.*, **17** 4 (1994), 429-439.

306. K. A. Gall et al., Atomistic simulations on the tensile debonding of an Aluminum–Silicon interface, *J. Mech. Phys. Solids*, **48** (2000), 2183-2212.

307. J. Glimm, and D. H. Sharp, Multiscale science: a challenge for the twenty-first century, *Siam News*, **30** 8 (1997), 1-7.

308. M. E. Kassner et al., New directions in mechanics, *Mech. Mater*., **37** (2005), 231-259.